NAZARBAYEV UNIVERSITY

Master thesis

Functional analysis of TYRO3 isoforms in bladder cancer cells

Student: Islana Ginayatova

ORCID: 0000-0001-9322-0296

Program: Master of Pharmacology and Toxicology

PI: Dr. Marina Kriajevskaia

Co-PI: Dr. Eugene Tulchinsky

A THESIS SUBMITTED

FOR THE DEGREE OF MASTER OF PHARMACOLOGY AND TOXICOLOGY

DEPARTMENT OF BIOMEDICAL

SCIENCES SCHOOL OF MEDICINE NAZARBAYEV UNIVERSITY

2024

DECLARATION

I hereby declare that the thesis is my original work, and it has been written by me in its entirety. I have duly acknowledged all the sources of information which have been used in the thesis. This thesis has also not been submitted for any degree in any university previously.

Student name: Islana Ginayatova
Signature: Islana Ginayatova
Date: 22.04.2024

TABLE OF CONTENTS

Abstract

Bladder cancer (BC) is the 10th most common cancer type both in men and women and its incidence increases with age. TYRO3 is increased in 50% of muscle invasive bladder cancer (MIBCs), and TYRO3 overexpression confers TYRO3 dependence on bladder tumor cells. The downregulation of TYRO3 was linked to a decrease in bladder cancer cell growth and TYRO3 knockdown caused bladder cancer cell cycle arrest. The utilization of distinct BC cell lines in the investigations may imply that inhibiting TYRO3 has distinct effects. This thesis work hypothesizes that alternatively spliced TYRO3 isoform 2 is present in the nucleus of T24 and RT112 bladder cancer cells and regulates gene expression. Molecular cloning techniques were used to construct the recombinant plasmid, which were further transfected into T24 and RT112 cell lines and expression of protein were analyzed by Western Blotting method. The results of the thesis project are thoroughly presented and future perspectives are described.

1. INTRODUCTION

1.1. Bladder cancer overview: epidemiology, risk factors and stage progression

Bladder cancer (BC) is the 10th most common cancer type both in men and women (Sung et al., 2021)World Cancer Research International, last accessed 17 October 2023). Bladder cancer incidence increases with age and is prevalent among men rather than women (Siegel et al., 2022). Overall, men have a three-fold higher prevalence of bladder cancer new cases and a 2.4 fold higher mortality rate (Siegel et al., 2023). The yearly incidence of new bladder cancer cases stood at 18.2 per 100,000 individuals, encompassing both men and women. The annual mortality rate was 4.2 per 100,000 men and women (NCI, SEER, last accessed 17 October 2023). In the US, the estimated death from urinary bladder cancer fell slightly from 17,100 to 16,710 between 2022 and 2023. At the same time, the estimated number of new cases increased slightly for both sexes, from 81,180 to 82,290.

The most well-known risk factor for bladder cancer is smoking, which is responsible for around half of cases in the United States. The risk of adverse health effects is particularly elevated among individuals employed in the dye, rubber, leather, and aluminum sectors, as well as painters and firefighters. Additionally, individuals residing in communities with increased

levels of arsenic in their drinking water, and those with congenital bladder abnormalities or long-term urinary catheters, are also at increased risk (Cancer Facts & Figures 2023). The symptoms through which bladder cancer can be detected include blood in the urine, frequent urination, and urination discomfort.

Bladder cancer is categorized into two types: muscle-invasive bladder cancer (MIBC) and non-muscle-invasive bladder cancer (NMIBC).

Non-Muscle Invasive Bladder Cancer refers to a specific subtype of bladder cancer that is localized inside the innermost layer of the bladder lining, without infiltrating the muscle wall. The condition commonly includes carcinoma in situ, T0, and T1 stages, exhibiting comparatively lower aggressiveness. The transurethral resection used for both treatment and detection of NMIB. While, intravesical therapy used to mitigate the likelihood of recurrence (Kaufman et al., 2009).

Muscle-invasive bladder cancer is characterized by its increased aggressiveness since it infiltrates the muscle layers of the bladder wall, frequently resulting in metastasis. The standard treatment modalities commonly employed in clinical practice include radical cystectomy, radiation therapy, and/or systemic administration of chemotherapeutic agents. The prognosis for this particular form of bladder cancer is typically less favorable in comparison to NMIBC due to a high likelihood of metastasis to other organs.

The most effective course of therapy and the likelihood of a positive outcome for the patient are determined by staging and grading (Compérat et al., 2022). Bladder cancer stages can be categorized as follows (Amin et al., 2017) (Figure 1):

When a cystectomy material has no detectable trace of transitional cell carcinoma, it is classified as stage pT0. Patients with bladder cancer MIBC may undergo neoadjuvant chemotherapy before radical cystectomy. Some patients may have a stage pT0 at the time of surgery without receiving neoadjuvant chemotherapy. Stage pTa refers to transitional cell carcinoma (TCC) without invasion. The histological grade is important for pTa bladder tumors. Urothelial carcinoma in situ (CIS) is a urothelial lesion characterized by abnormal urothelial cells without invasion. Cystectomy specimens with urothelial CIS but no invasive component are classified as pTis stage. Urothelial carcinoma is classified as stage pT1 when it has invaded the

lamina propria but not the muscularis propria. The tumor infiltration into the muscularis propria is a characteristic of urinary bladder cancer in stage pT2. It can be further subdivided based on the tumor invasion. Stage pT3 bladder cancer occurs when the tumor invades the soft tissues around the bladder, specifically the fat outside the muscularis propria. There are two subcategories within pT3, which are pT3a and pT3b. pT3a refers to the microscopic invasion of soft tissue, while pT3b refers to the macroscopic invasion of soft tissue. When a tumor spreads beyond the bladder and invades nearby organs, it is classified as stage pT4. There are two subcategories, pT4a, and pT4b, which describe different types of direct invasion in the body (Magers et al., 2019).

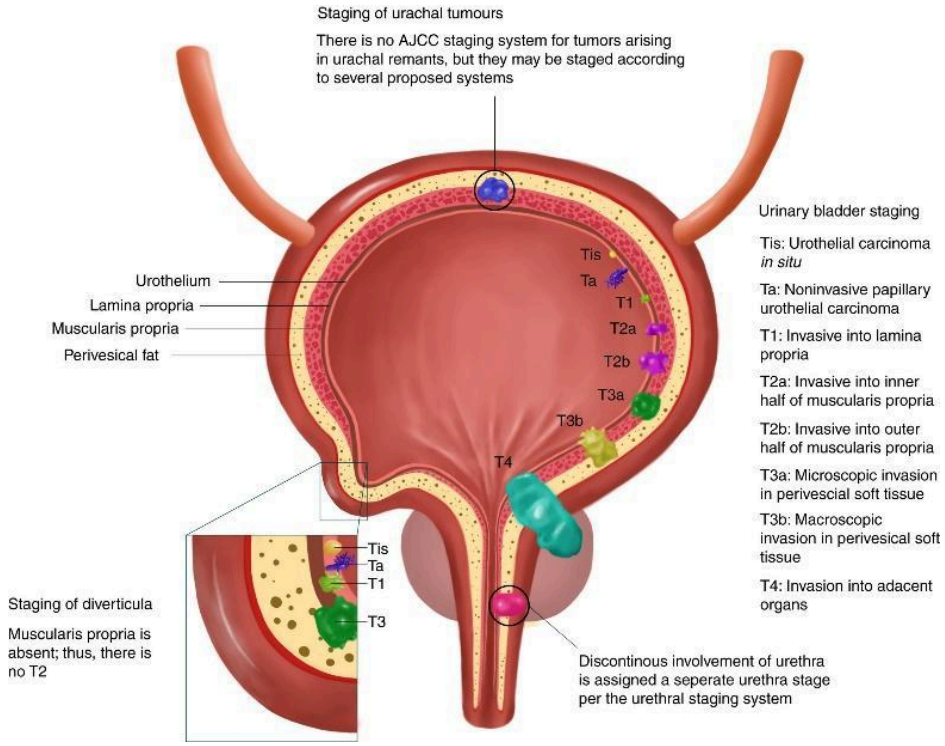

Figure 1. The visual depiction of the bladder exhibiting various stages of cancer. Reprinted from Magers et al., 2019.

1.2. TAM receptors in cancer

The acronym of the TAM family originates from the initial letter of its three members, namely Tyro3, Axl, and Mer (Lemke, 2013). TAM family is a receptor tyrosine kinase (RTK)

and members of the family were discovered under different names and grouped into one family in early 90s. They were confirmed into a family of orphan RTKs after isolation of full length cDNAs. Subsequently, growth arrest-specific 6 (Gas6) and Protein S (Pros1) were discovered to be the two ligands that bind and activate the TAMs.

TAM kinases are composed of three domains: intracellular, extracellular, and a single-helix transmembrane domain(Crosier et al., 1994). Two fibronectin type III domains and two Ig domains make up the extracellular domain, whereas the domain in the cytoplasm is involved in the activity of kinase and serves as a binding site for other molecules (Smart et al., 2018). The significance of these motifs lies in their association with cell-cell interactions. Also, they exhibit a resemblance to the neural cell adhesion molecule (NCAM) structure (Yamagata et al., 2003). The inclusion of a conserved KW(I/L)A(I/L)ES motif in the kinase domain is another distinguishing trait of this family of tyrosine kinases. In this sequence, amino acids at positions 3 and 5 are identified as isoleucine (I) in the proteins MERTK and AXL, whereas leucine (L) is seen at position 5 in the protein TYRO3 (Graham et al., 2014; Linger et al., 2008).

Structure of Tam receptors ligands (vitamin K-dependent proteins Gas6 and ProS) are as follows: The two ligands exhibit a similar domain structure, consisting of an γ-carboxyglutamic acid domain, a loop region, 4 epidermal growth factor (EGF)-like repeats, and a sex hormone-binding globulin (SHBG) domain (Hafizi & Dahlbäck, 2006; Pastore et al., 2019; van der Meer et al., 2014). The SHBG domain consists of two globular laminin G-like domains and is responsible for facilitating the interaction between ligands and receptors. Gas6 has the ability to bind to all members of TAM receptors, namely Tyro3, Axl, and Mer, whereas ProS exhibits binding affinity only towards Tyro3 and Mer receptors. However, ProS demonstrated that it has the ability to physically interact with and stimulate the activation of Axl in cultures of glioma spheres (Sadahiro et al., 2018).

A tetrameric complex with a 2:2 stoichiometry is produced when a ligand and a receptor connect (Sasaki et al., 2006). The optimal receptor activation requires concurrent ligand binding and the existence of a membrane that presents PtdSer, for instance, in cells undergoing apoptosis, enveloped viruses, or phosphatidylserine (PtdSer) liposomes (Lew et al., 2014). Activation process results in the autophosphorylation of tyrosine residues that are located in close proximity to a conserved region within the cytoplasmic domain. Therefore, this event

improves catalytic efficiency, which makes it easier to recruit and phosphorylate many signaling molecules.

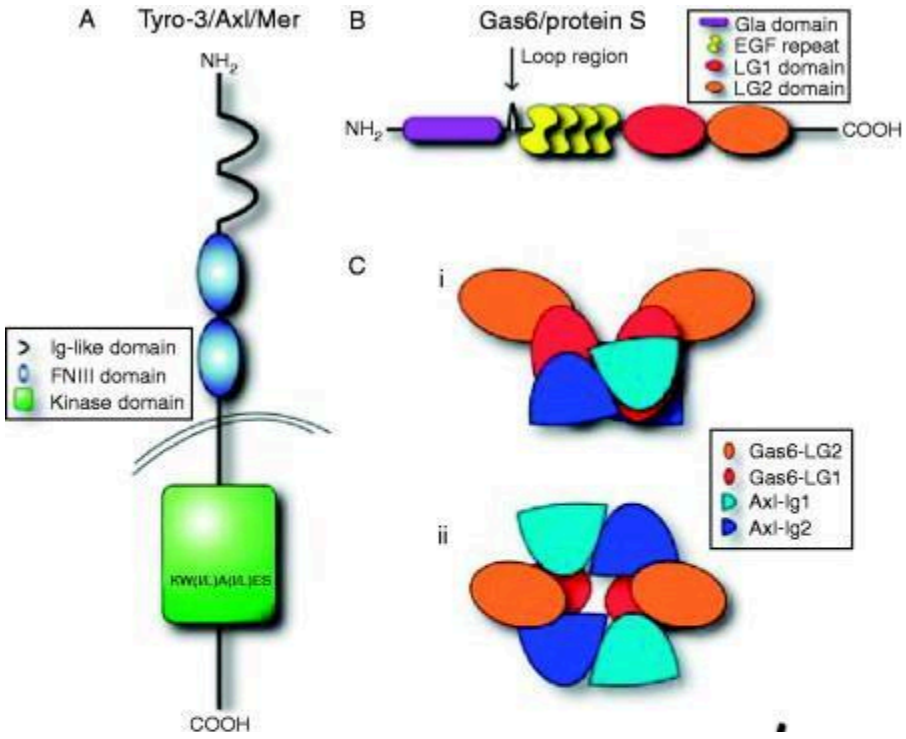

Figure 2. The structure of the TAM (Tyro3, Axl, Mer) receptor and their ligands (ProS1 and Gas6). Reprinted from Linger et al., 2008.

The presence of TAM receptors on cancer cells are apparent. However, information about Tyro3 and its presence in human cancer is insufficient. Several forms of cancer, including gliomas, colorectal malignancies, leukemias, and breast cancers, have been linked to increased expression of TAM signaling components (Lemke, 2013). It has also been found that Axl activation and up-regulation is a clinically important part of non-small-cell lung cancer that does not respond to EGF and PI3K inhibitor treatments (Lemke, 2013; Wee & Wang, 2017; Weng et al., 2019). Expression of Axl and Gas6 is often more strongly linked to metastasis than to growth of the original tumor (Shibue & Weinberg, 2017). Inhibitor of Axl RTK has demonstrated effectiveness in reducing cancer metastasis, rather than inhibiting the growth of the initial tumor, in experimental mice models of breast cancer (Graham et al., 2014).

There are different tumor growth mechanisms that have been studied. Particularly, TAM receptors have been found in natural killer (NK) cells, invading myeloid-suppressor cells, macrophages, contributing to cancer growth because immune cells directly regulate evasion into the immunity (Paolino et al., 2014). TAM receptors promote the expression of the immunological checkpoint protein programmed cell death ligand 1 (PD-L1) in tumor cells, allowing immune escape (Kasikara et al., 2017). Some cancers release Pros1, which may connect to Mer and Tyro3 on local macrophages, reducing anticancer adoption ability.

Tam receptors are converted to soluble TAM receptors by proteolytic cleavage by enzymes such as metalloproteinase or metallopeptidase (Uehara et al., 2022). Soluble TAM Receptors undergo translocation from the cellular membrane in order to engage in recycling processes. These receptors function as decoy receptors for the Gas6 and ProS1 ligands, hence hindering the phagocytic activity of macrophages.

Soluble TAM receptors can be generated by alternative splicing (Biesecker et al., 1995; Schulz et al., 1993) or proteolytic cleavage (Thorp tyrosine kinase et al., 2011) and represented as sTyro3, sAxl, and sMer. The alternative splicing impacts both the localization and functionality of receptors, whereas the proteolytic cleavage renders receptors inactive. It has been observed that circulating receptors possess the ability to bind ligands, therefore functioning as decoys (Sather et al., 2007). The presence of circulating receptors can impact signaling pathways and disrupt the process of phagocytosis (Seitz et al., 2007). A correlation exists between deviant TAM receptor levels and several pathological conditions. The reduction of TAM receptor activity is a reason for autoimmune disorders. In contrast, elevated TAM expression is associated with resistance to chemotherapy, metastasis, and increased death rates among cancer patients.

TAM signaling can be restricted by soluble TAM receptors, which may block accessible ligands (Costa et al., 1996). Highly affinitous binding of Gas6 to engineered Axl decoy receptor (Kariolis et al., 2014) neutralizes ligands and inhibition of Gas6/Axl signaling, metastasis, and cancer development.

1.3. TYRO3

The TYRO3 gene in humans is found on chromosome 15q15.1 and comprises a total of 19 exons. Based on sequence analysis, it is anticipated that exons 1-9 will be responsible for encoding the extracellular domain. The transmembrane region may be encoded by exon 10, and the intracellular domain by exons 11-19. According to Hubbard et al. (2009), exons 12-19 may contain the genetic information necessary for encoding the tyrosine kinase domain, which is located inside the intracellular region(Jacobsen et al., 2010).

The molecular weight of the human TYRO3 protein is 98 kDa, with 890 amino acids; however, because of post-translational modifications, the actual molecular weight varies from 120 to 140 kDa (Brown et al., 2012). There are two known TYRO3 splice variants, and a third is predicted to include exons 2A, 2B, or 2C. Since a signal peptide is encoded by these exons, Tyro-3's post translational processing, localization, and function may be affected by the existence of these splice variants (Linger et al., 2008).

Alternative splicing leads to the generation of three distinct splice variants. Isoform I encompasses exon 2A, Isoform II comprises exon 2B, and Isoform III harbors exon 2C. All three splice variants encode a transmembrane TYRO3 protein; however, they exhibit variations in the signal peptide sequence located at the amino terminus (Jacobsen et al., 2010)(Figure 3).

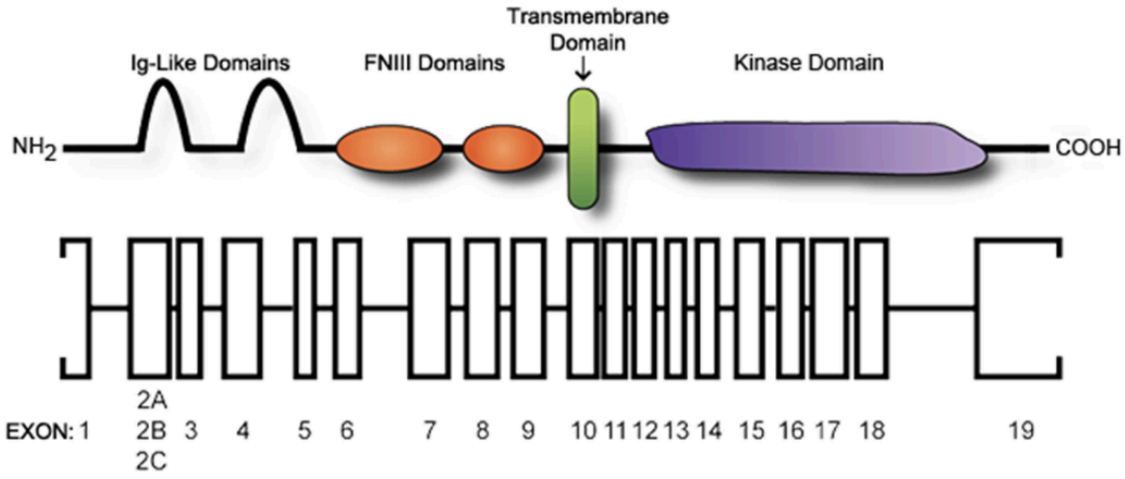

Figure 3. The schematic representation of the TYRO3 gene. Information of genetic makeup: boxes represent exons, while lines represent introns. Reprinted from Jacobsen et al., 2010.

TYRO3 is naturally expressed in several tissues, with the nervous system being the most prominent: cerebral cortex, amygdala, hippocampus, etc (Mark et al., 1994; Schulz et al., 1993). Numerous cancers have been reported to express TYRO3, including colon, breast, lung, liver cancers, schwannoma and many more. TYRO3 was often overexpressed in comparison to the equivalent normal tissues. For instance, in human liver cancer cell line compared to a normal hepatocyte cell line, and in around 40% of patient samples with hepatocellular carcinoma, TYRO3 mRNA levels were higher by two-fold or more than in the surrounding normal liver tissue(Duan et al., 2016).

TYRO3 mutations in cancer are of particular interest. Although they have been identified in human cancers, no functional research has been done to determine the possible importance of these mutations. Colon cancer, lung cancer, and melanoma have all been linked to mutations within the kinase domain (Ding et al., 2008; Seshagiri et al., 2012; Wagle et al., 2014). Melanoma, pancreatic cancer, and colon cancer have all been linked to cytosolic domain alterations(Jiao et al., 2014). Premature stop codons resulting from mutations in the extracellular and transmembrane domains were found in lung cancer and melanoma.

1.4. TYRO3 in bladder cancer

According to recent studies, TYRO3 is increased in 50% of MIBCs, and TYRO3 overexpression confers TYRO3 dependence on bladder tumor cells (Silina et al., 2022). According to, bladder cancer cell proliferation and invasion are stimulated by overexpression of GAS6, a potent TAM ligand (Mao et al., 2020). The downregulation of GAS6 and TYRO3 was linked to a decrease in bladder cancer cell growth. Studies established that TYRO3 knockdown caused bladder cancer cell cycle arrest (Silina et al., 2022). The utilization of distinct BC cell lines in the investigations may imply that inhibiting TYRO3 and GAS6 has distinct effects, which is conceivable given that GAS6 is a potent receptor that binds to AXL and MERTK and Protein S1, an additional TAM ligand, may be involved (Varnum et al., 1995).

Recent studies (Dufour et al., 2019) have found that all TAM receptors are expressed in BC cell lines. However, the TYRO3 is the receptor primarily responsible for cell viability. TYRO3 was discovered to be the most frequently expressed TAM receptor in a study that looked at the

protein expression of TAM receptors in human urothelial bladder cancer (UBC) cell lines. Due to the greater impact of TYRO3 silence compared to AXL knockdown, therapeutic targeting of TYRO3 may be feasible. The study also discovered that the most susceptible cell lines to TYRO3 depletion and TAM receptor inhibitors were MGH-U3 and RT112, which express solely TYRO3.

Tumor development was inhibited in both in vitro and in vivo settings when TYRO3 was knocked out (Dufour et al., 2019). Depletion of TYRO3 dramatically reduced bladder cancer cell viability and tumor growth, indicating a function in clonogenic cell survival. TYRO3 siRNA treatment inhibited tumor development, revealing TYRO3 as a possible therapeutic target.

TYRO3 in depleted state induces anti-tumor pathways and cell death, whereas inhibit malignancy proliferation. Study (Dufour et al., 2019) discovered 284 genes that were expressed differently following TYRO3 knockdown in MGH-U3, RT112, and UM-UC-5 cells treated with three distinct TYRO3 siRNAs. It revealed critical molecular and cellular activities, as well as upstream regulators/transcription factors, that show substantial changes when TYRO3 is knocked out. Cell survival and cell cycle were dramatically suppressed, but cell death and apoptosis were significantly increased. TYRO3 depletion was projected to downregulate or upregulate the top ten transcriptional regulators encoding critical regulators of the cell cycle and cell survival. FOXM1 and CYCLIN D1 levels were reduced in MGH-U3, RT112, and UM-UC-5 cells after TYRO3 depletion, according to Western blot analysis. Because the western blot results were verified in two different TYRO3-dependent cell lines, these molecular pathways are of broad interest.

2. Aims

To express and analyze localization of TYRO3 isoforms in bladder cancer T24 and RT112 cell lines.

Hypothesis: Alternatively spliced TYRO3 isoform 2 is present in the bladder cancer cell lines nucleus and regulates gene expression.

Objectives:

- To construct a primer design for TYRO3 isoforms with a specific tag
- Molecular cloning of the recombinant plasmid containing TYRO3 isoforms
- Cell culture work with T24 and RT112 cell lines
- Transfection of TYRO3 Isoform 1 and 2 in T24 and RT112 BC cell lines
- Analysis of TYRO3 Isoform 1 and 2 expression by Western Blotting
- Analysis of TYRO3 Isoform 1 and 2 localization by Immunofluorescence

3. MATERIALS & METHODS

3.1. Materials

For Molecular cloning

Plasmids

- pIRES-GFP-TYRO3 kindly provided by Dr. Kriajevskaia
- pIRES-puro2 kindly provided by Dr. Kriajevskaia

Primers kindly provided by Dr. Tulchinsky

Primers	Direction	Sequence
F-PIRES 1	Forward	5’-TTAGCTAGCATGGCGCTGAGGCGGAGCA-3’
R-PIRES	Reverse	3’-CTAGAATTCAGCATAATCTGGAACATCATATGGATAACA GCTACTGTGTGGCAG - 5’

Table 1. Primers for TYRO3 Isoform 1

Primers	Direction	Sequence
F-PIRES 2	Forward	5’-TTAGCTAGCATGGGAGCCCCGGTGAAGC-3’
R-PIRES	Reverse	3’-CTAGAATTCAGCATAATCTGGAACATCATATGGATAAC AGCTACTGTGTGGCAG - 5’

Table 2. Primers for TYRO3 Isoform 2

Competent cells

XL-1 Blue competent cells kindly provided by I.Malikova and DH5-alpha competent cells kindly provided by Dr. Kriajevskaia

Primers for sequencing

TYRO3 isoforms 1 & 2

Primers	Direction	Sequence	Company
TYRO seq 1	Forward	5'- TCAGCCTGAAGTCAGTGGAG-3'	Thermofisher Scientific
TYRO seq 2	Forward	5'-TTCAGGCCTCATCTTGGAGTGG-3'	Thermofisher Scientific
TYRO seq 3	Forward	5'-TTGCATGAAGGAGTTTGACC-3'	Thermofisher Scientific
TYRO seq 4	Forward	5'-GGAGTGTATGGAGGACGTGT-3'	Thermofisher Scientific
TYRO seq rev	Reverse	5'-CACAGCCTCACAAGACAGT-3'	Thermofisher Scientific

Table 3. Primers for sequencing of TYRO3 Isoform 1 and 2

For cell culture work

Cell lines:

T24, R112 and RT112-FRA1-HA bladder cancer cell lines were provided by the EMT group.

Antibodies:

Primary antibodies:

- HA-probe Antibody (Y-11): sc-805 (Santa Cruz)

Secondary antibodies:

- Anti-rabbit Alexa fluor 488 (Invitrogen)
- Goat anti-rabbit HRP (ab6721, Abcam)

3.2. Methods

3.2.1. Molecular Cloning

PCR amplification

For molecular cloning, the primer and plasmids design was done (Refer to Results section). Annealing temperature for forward and reverse primers for TYRO3 Isoform 1 and 2 were calculated (Tm= 63C). To make an Isoform 1 and Isoform 2 clones, pIRES-GFP-TYRO3 (10 ng) were PCR amplified with 1 ul of respectives primers (F-PIRES1, C=134 µM diluted to 10 uM; F-PIRES2 , C=167 µM diluted to 10 uM; R-PIRES, C= 121 µM diluted to 10 uM), 2X KOD Hot start Master mix (71842, Merck) and topped up with distilled water to 20 ul. PCR program were as follows:

- Initial Denaturing: 95 ˚C, 3 min
- Final denaturation: 95 ˚C, 30sec
- Annealing: 63 ˚C, 1 min
- Extension: 72 ˚C, 3 min
- Repeat steps 2-4, 30x
- Final extension: 70 ˚C, 3 min
- Infinite hold: 4 ˚C

The PCR products were applied onto a 0.8% agarose gel in the TAE buffer , settings: 80V for 20-25 min. 0.8% agarose gel was prepared using the following steps: 0.4 g of agarose powder was dissolved in 50 ml of 1X TAE (Tris-acetate-EDTA) buffer (pH 8.0). Then, 1μL (or less) of ethidium bromide was added, ensuring to avoid bubbles. The agarose gel was poured and the comb was gently inserted. After letting it cool, a 1X TAE buffer was applied. Lambda DNA digested with EcoRI-HF (high fidelity) and HindIII restriction enzymes were used as a DNA marker (C=0.2 ug/ul).

After the amplification, PCR samples were purified using the E.N.Z.A nucleic acid purification kit: PCR cleanup, dimers removal protocol. The reaction mixture was adjusted to 200 μL with distilled water. After adding Binding Buffer and ethanol, the mixture was transferred to a DNA Purification Micro Column, centrifuged, and washed with Prewash and Wash Buffers. Residual ethanol was removed through centrifugation. Elution Buffer was added to elute DNA, and the purified DNA was stored at -20°C. Concentration of purified DNA was determined using the NanodropTM 2000C spectrophotometer.

Digestion

Obtained inserts and vector were digested with EcoRI and NheI restriction enzymes to create sticky ends for ligation. Digestion mixture contained 1.3 ul of EcoRI-HF and NheI, 3 ul of 10X rCutSmart Buffer (B6004S, NEBioLabs), insert or vector, and distilled water to top up to 30 ul.

After digestion, heat inactivation of restriction enzymes was carried 65°C for 20 minutes.

Afterwards, analyzed on 0.8% agarose gel. The mixture was incubated on 37℃ for 30 min. Purification of digested pIRES-puro2 vector, TYRO3 Iso-1 and 2 were done with the E.N.Z.A nucleic acid purification kit: General DNA cleanup from enzymatic reactions protocol.

Ligation

For ligation T4 DNA ligase (Part# 9PIM180, Promega) was used. The following reaction was assembled in a sterile microcentrifuge tube in a molar ratio insert:vector 1:3, total 10 μL:

TYRO3 Isoform 1 and 2

- 1 µL of vector DNA, 50-100 ng/µL
- 1 µL of TYRO3 Iso-1 or 2, 17-20 ng/µL
- 5 µL of Ligase 2X Buffer
- 0.5-1 µL of T4 DNA Ligase
- Deionised water to top to 10 µL

Vector self-ligation

- 1 µL of vector DNA, 50-100 ng/µL
- 5 µL of Ligase 2X Buffer
- 0.5-1 µL of T4 DNA Ligase
- Deionised water to top to 10 µL

The reactions were incubated at room temperature for 3 hours or overnight at +4

Transformation

XL-1 Blue and DHL5a E.coli cells were used. All the eppendorf tubes and reagents were pre chilled in an ice bucket. 20 ul of XL-1/ DHL5a were added along with 2 uL of ligation mixtures or controls into the tubes. They were kept on ice for 30 minutes. Next, they were placed in a thermostat at 42°C for 45 seconds and then returned to ice for 3 minutes. Following this, LB broth was added, making the solution 10 times more, totaling 200 uL. The mixture was then kept on a thermostat at 37°C , 300 rpm for 1 hour. Finally, 100 uL was spread on agar plates with 50 ug/mL ampicillin and incubated at 37 C overnight.

After overnight incubation, up to 12 colonies transformed with vector and TYRO3 Iso-1 and Iso-2 inserts were cultured in a 15 ml falcon tube with 1 ml of LB broth with 50 ug/mL ampicillin. The tubes were incubated overnight on a shaker set at 37 C and 300 rpm.

Plasmid isolation

The plasmids were isolated by using E.Z.N.A. Plasmid DNA Mini Kit (D6942-02, Omega) after overnight culturing. The isolated plasmids were loaded on 0.8% agarose gel with a self-ligated vector as a negative control. Isolates exhibiting bands that differed from negative control were further evaluated.

The colony PCR was done to screen the maximum amount of colonies to verify desired insert is present and was done as follows. Sterile PCR tubes were used with 6 µL of autoclaved distilled water added. Colonies were resuspended in the water, resulting in a cloudy solution. Three microliters of this solution were used for a 10 µL PCR reaction. A master mix containing 2X REDTaq® ReadyMix™ (R2523, Sigma Aldrich), F-PIRES 1, R-PIRES was prepared. Seven microliters of the master mix and 3 µL of the colony solution were combined for each PCR reaction. The samples were then run on the PCR machine, and the resulting products were analyzed on a 0.8% agarose gel. A small amount of the control was also tested to avoid signal interference.

The concentrations of selected isolated plasmids were measured on the NanodropTM 2000C spectrophotometer. The clones obtained was treated with EcoRI and NheI and incubated at 37 ℃ for 1 hour. The digested clones were compared with EcoRI and NheI treated pIRES-TYRO3-GFP and pIRES-puro2 vector plasmid. The digestion mixtures were loaded on 0.8% TAE agarose gel and run at 80V for 20 minutes. TYRO3 Iso 1 and 2 clones with identical bands with pIRES-TYRO3-GFP and pIRES-puro2 vector after EcoRI and NheI digestion were selected and incubated in 200 mL LB broth with 50 ug/mL ampicillin for further overnight incubation on shaker at 37 ℃, 300 rpm. The TYRO3 Iso 1 and 2 clones plasmid was isolated from 200mL bacterial culture using E.N.Z.A Plasmid DNA Maxi Kit. Nanodrop spectrophotometer was used to measure the concentration.

3.2.2. TYRO3 Isoforms 1 and 2 Sequencing

The Sanger sequencing method was used to confirm the isoforms. TYRO3 Isoform 1 and 2 were amplified by five primers (forward primers: TYRO seq 1, TYRO seq 2, TYRO seq 3,TYRO seq 4 and reverse primer: TYRO seq rev). Each PCR mixture contained 2 µl of 5X Big Dye Terminator, 100 ng of TYRO3 Isoform 1 and 2, 1µl of respective primer and nuclease free water to top up to 10 ul. PCR program:

- Initial Denaturing: 95 ˚C, 1 min
- Final denaturation: 95 ˚C, 10 sec
- Annealing: 63 ˚C, 5 sec
- Extension: 60 ˚C, 4 min
- Repeat steps 2-4, 25x
- Infinite hold: 4 ˚C

The PCR product was precipitated for sequencing using a freshly prepared sodium acetate solution (37.5 µL of 3M sodium acetate (pH 4.6-5.2), 782.5 µL of 95% ethanol, and 180 µL of dH2O). A 100 µL portion of this solution was added to 20 µL of the sample, allowed to incubate for 30 minutes at room temperature, and then centrifuged at 13200g for 30 minutes at +4°C. The supernatant was carefully removed, and 80 µL of 75% ethanol was added to each sample. After repeating the centrifugation step, the supernatant was removed again, and the DNA pellet was completely dried at room temperature for approximately 30 minutes. Next, 14 µL of Hi-Di formamide was added and vortexed into the dried pellet. The mixture was left at room temperature for 20 minutes, then denatured at 95°C for 2 minutes, followed by cooling on ice for 5 minutes. The samples were either stored in the -20°C freezer or proceeded directly for sequencing. DNA sequence analysis was performed using the Applied Biosystems ABI 3500 Genetic DNA Analyzer at Nazarbayev University Core Facilities. Quality analysis and chromatograms were read by the Snapgene software and sequence check was performed via BLAST database.

3.2.3. Cell culture work

Before starting cell culture work all the reagents were prepared. Complete DMEM medium was prepared: High-glucose DMEM with 10% Fetal Bovine Serum, 1% Pen/Str, 1% non-essential amino acids, 1 % sodium pyruvate and stored in +4 fridge. PBS tablets (1 tablet per 200 ml) were dissolved in distilled water and autoclaved. Freezing medium was prepared: High-glucose DMEM was supplemented with 50% FBS and 10% DMSO.

The frozen vials containing human bladder cancer cells (T24, RT112, and RT112-FRA1-HA) were thawed and centrifuged at 1000 rpm for 5 minutes with 9 ml of complete DMEM. The resulting pellet was then resuspended in 1 ml of complete DMEM. The cell suspension was transferred into a T75 flask with 12 ml of medium. If the pellet was small, the cell suspension was instead applied into a T25 flask with 5 ml of medium. The flasks were then placed into the CO2 incubator (37 C and 5% CO2), and the confluency of the cells was checked the next day. Once the cell confluency reached 80-90%, the cells were passaged into another flask. When the passaged cells reached 80% confluency, cells from one of the flasks were selected to be frozen in labeled cryovials using freezing medium and stored at -80°C. Cells from another flask were stained with trypan blue dye and counted using the Countess II FL Automated Cell Counter.

3.2.4. Transfection by lipofectamine 3000

The 12 well plate was used to test a transfection efficiency and all reagents were calculated, according to manufacturer instructions (L300000, Thermo Fisher Scientific).

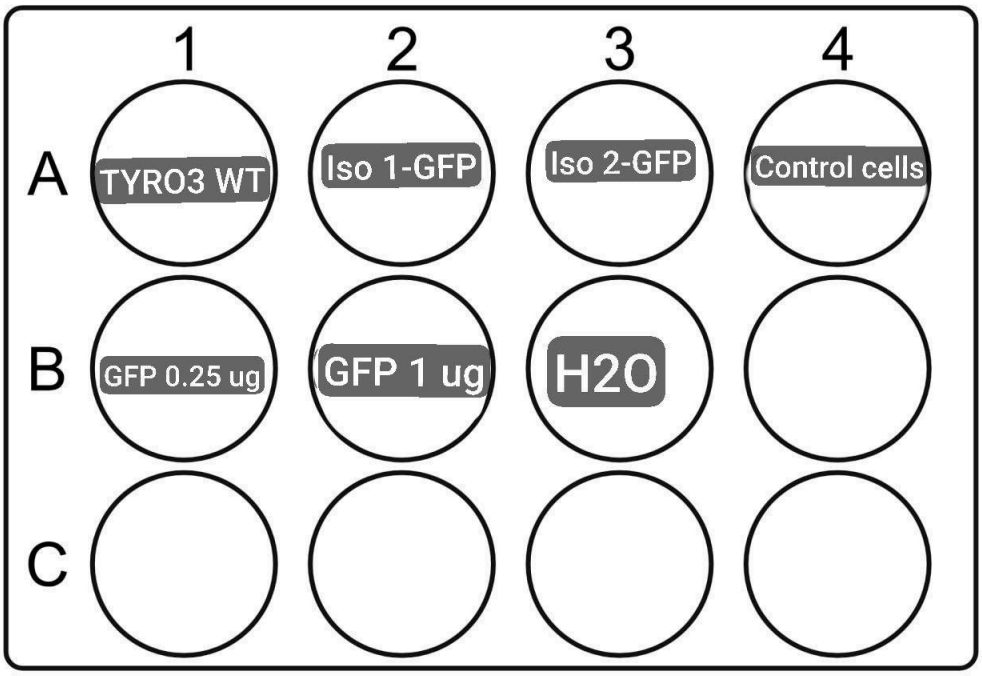

Figure 4. The scheme of transfection with EGFP, TYRO3 Isoforms 1 and 2 to 12 well-plate

After confirming transfection, a 6-well plate was used. It was labeled with plasmid DNA and controls. 3*10^5 cells in 2 mL of complete medium were seeded onto the 6-well plate and incubated for 24 hours. Following the incubation period, the cells underwent a wash with PBS, and then the medium was changed.

In preparation for transfection, two tubes were prepared. Tube 1 contained 125 µL of Opti-MEM and 5 µL of Lipofectamine 3000, while tube 2 contained 125 µL of Opti-MEM, 2 µg of plasmid DNA/sample, and 5 µL of P3000 enhancer. These tubes were mixed and incubated at room temperature for 15 minutes. The resulting mixture was then added to the cells in the 6-well plate, and the plate was gently swirled to ensure an even distribution of the complex throughout the well.

Transfection efficiency was assessed by observing GFP fluorescence using a ZEISS Primovert inverted microscope after 24 and 48 hours of incubation.

3.2.5. Immunofluorescence

Immunofluorescence protocol aimed to visualize the localization of TYRO3 Isoforms 1 and 2. The coverslips 26x76 mm (09-2000, Bio-Optica) were placed at the bottom of a 6-well plate and exposed to UV light for 15 minutes. Then, 3*10^5 cells were added with 2 ml of complete medium to each well and incubated until reaching 80% confluency, at which point transfection was conducted. The transfected cells underwent two washes with PBS before being fixed with 2 ml of 4% paraformaldehyde in PBS for 15 minutes within a fume hood.After another round of PBS washing, 2 ml of 0.1% PBT (50 uL TritonX-100 + 50 ml PBS) was applied for 15 minutes.

Following three PBS washes, the cells were incubated with a primary antibody at room temperature in a wet chamber for 1 hour. The antibody (HA probe, diluted 1:100) was prepared in DMEM, and approximately 150-200 ul was added to each slide. After three PBS washes, a secondary antibody (AlexaFluor 488 donkey anti-rabbit, Invitrogen, diluted 1:500 in DMEM) was applied for 1 hour, 6 well plate was covered in aluminum foil.

Next, the samples were washed three times with PBS and treated with PBS containing DAPI (ThermoScientific #62248, diluted 1:5,000) for 5 minutes, 6 well plate was covered in aluminum foil. Following 2-3 additional PBS washes, mounting media (Fluoromount-G, Invitrogen #CO-4958-02) was applied to the coverslips using a loop. Excess liquid was removed, and the coverslips were sealed with nail polish.

3.2.6. Western Blotting

Protein lysates preparation

The protein lysates were prepared by growing cells in 10 cm culture dishes until they reached 80% confluency. The cells were then washed three times with PBS and lysed by adding 800-1000 µl of 1X Laemmli buffer (1% Sodium Dodecyl Sulfate (SDS), 10% glycerol, and 0.05 M Tris with pH of 6.8) and pipetting. Subsequently, the cells were scraped to one side of the dish and transferred to an Eppendorf tube.

The lysates were heated at 95°C for 5 minutes and subsequently cooled to room temperature. After cooling, the samples were sonicated at an amplitude of 20 for 15 seconds using the Q55 Sonicator. The concentration of the samples was determined using the bicinchoninic acid (BCA) assay, and the remaining lysates were stored at -20℃.

BCA assay

Standards for the BCA assay were prepared using a fresh vial containing 2 mg/ml of BSA standard. This standard was then diluted to create eight different concentrations (2000, 1000, 750, 500, 250, 100, 50, and 25 µg/ml) in the 4X Laemmli buffer.

The working reagent (WR) was prepared by combining BCA solution A and solution B in a 50:1 ratio, with the volume calculated based on the number of wells in the 96-well plate. Next, 20 µl of each standard and protein samples were pipetted into individual wells of the 96-well plate, followed by the addition of 200 µl of WR to each well. Following that, the plate was shielded from light by covering it with aluminum foil and then placed in an incubator at 37°C for 30 minutes. Subsequently, the plate was allowed to cool down to room temperature.Absorbance readings were taken at 540 nm using a plate reader. All data obtained were used to generate a standard curve and calculate the protein concentrations in the samples.

Buffer preparation

10X Running buffer (30 g Tris base, 144 g glycine, 100ml 10% SDS, topped up to 1L with H2O), 1X Running buffer (10X running buffer diluted 1:9), 10X Transfer buffer (30 g Tris base, 144g glycine topped up to 1L with H2O), 1X Transfer buffer (100 ml 10X Transfer buffer, 200 ml 96% ethanol, made up to 1 L using distilled water), 20X TBS (121.14g Tris base, 175.32 g NaCl, 500 ml distilled water; pH adjusted to 7.65 using pH meter and gradual addition of HCL and made up to 1 L with dH2O), 1X TBST (1 ml Tween 20, 50 ml 20X TBS, topped up to 1 L with dH2O).

SDS-PAGE

A 12% resolving gel was prepared using the following components: 4 ml of 30% Polyacrylamide, 3.3 ml of dH2O, 2.5 ml of 1.5M Tris buffer (pH 8.8), 0.1 ml of 10% SDS, 0.1 ml of 10% APS (248614-500G, Sigma-Aldrich), and 4 ul of TEMED (T9281-50mL, Sigma-Aldrich). This mixture was poured into a pre-assembled SDS-PAGE apparatus and allowed to solidify. Simultaneously, a 5% stacking gel was prepared using the following components: 0.33 ml of 30% Polyacrylamide, 1.4 ml of dH2O, 0.25 ml of 1M Tris buffer (pH 6.8), 20 ul of 10% SDS, 20 ul of 10% APS, and 2 ul of TEMED. TEMED was added when the gel was ready to be poured, as it initiates the gel setting process. After stacking gel was poured, combs were immediately placed.

The glass plates containing the gel were placed into the apparatus, and a buffer dam was used if only a single gel was being used. Subsequently, a 1X running buffer was used, making sure to cover the wells. Lysates were prepared by mixing with a dye containing 50% 2-mercaptoethanol and 50 % bromophenol blue. The dye was applied at the ratio to 1:25. These samples were then heated on a 94°-98° C heat block for 5 minutes. Following this step, the combs were taken out, and 3 µl of protein ladder (P7719S, NEB Biolabs) along with prepared samples (adjusted to contain 10-20 µg of protein) were loaded into the wells. The gel was then run at 120V for 1 hour.

Western Blotting

Following SDS-PAGE, the gel was removed from the cassette and the stacking gel was gently cut off. Filter paper, sponges and transfer cassette were submerged in the tray containing 1X transfer buffer, ensuring all components remained wet. The polyvinylidene difluoride (PVDF) membrane (IPVH85R, Millipore) was activated beforehand by soaking it in 96% ethanol before positioning it atop the gel. Then, western sandwich was assembled into the tank as follows: cassette black side facing down, sponge, filter paper, gel, activated membrane, filter paper, sponge, cassette with 1X transfer buffer and run for 18 hours at 20 V.

Following this, the membrane was immersed in Ponceau solution for 3-5 minutes. Subsequently, the membrane was thoroughly washed with TBST and put in 5% milk/TBS solution for 1 hour with gentle agitation. Washing with TBST was repeated. Meanwhile, the primary antibody (HA-probe antibody (Y-11): sc-805, Santa Cruz) was prepared at a dilution of

1:200 by combining 15 ul of the antibody with 3 ml of 3% BSA/1X TBST. Following that, the membrane was cut into needed sizes (FRA1-HA 37-38 kDa and TYRO3-HA 90-130 kDa) and pieces of membranes were put into a sealed plastic bag with primary antibody for 1 h with gentle agitation. Washing with TBST was repeated and membranes were put into the secondary antibody for again 1 h with gentle agitation. 2 ul of goat anti-rabbit HRP were mixed with 14 ml of 5% milk. Washing step with TBST repeated and membranes analyzed with a BioRad Chemiluminescence imaging system. Right before switching the apparatus, ECL solution in the ratio 1:1 can be applied onto the membrane.

4. RESULTS

4.1. Primer design

Primers for cloning of TYRO3 isoforms 1 & 2 fused with HA-tag were kindly Tm (melting temperature) calculation was done to establish the Ta (annealing temperature).

Tm calculation:

F-PIRES-1 5'- TTAGCTAGCATGGCGCTGAGGCGGAGCA-3'

Overhang	NheI	start	sequence

Tm = 69.3 + 0.41(%CG) – 650/primer length or 4 (G + C) + 2 (A + T)

First amplification:

Primer length = 19

%GC = 13/19*100 = 68.4

F-PIRES1 Tm= 4(13)+2(6)= 64 C or Tm= 69.3+(0.41 x 68.4%) –(650/19)= 63.13 C

F-PIRES 2 5'-TTAGCTAGCATGGGAGCCCCGGTGAAGC-3'

First amplification:

Primer length = 19

%GC = 12/19*100 = 63.158

F-PIRES 2 Tm= 4(12)+2(7)= 62C or Tm= 69.3+(0.41 x 63.158%)-(650/18)= 60.98 C

R-PIRES

CTAGAATTCAGCATAATCTGGAACATCATATGGATAACAGCTACTGTGTGGCAG

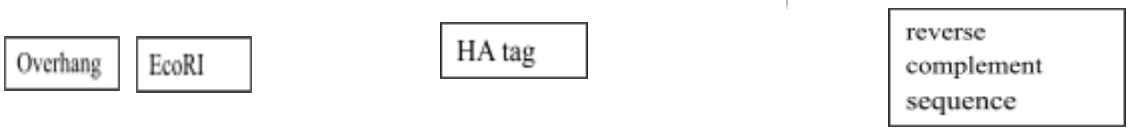

Primer length = 18

%GC = 10/18*100%=55.5

R-PIRES Tm = 69.3+(0.41x 55.5)–(650/18) = 55.94 C or 4(10)+2(8)=56 C

4.2. Primer design for cloning in pcDNA of TYRO3 isoforms 1 & 2 fused with myc tag

Restriction enzymes EcoRI and XhoI exhibit no cut sites within the pIRES-GFP-TYRO3 sequence and have one cut on pIRES-puro2 plasmid, making them optimal candidates for primer design.

Forward primer: overhang- EcoR1- TYRO3 sequence

Reverse primer: Myc-overhang- XhoI- TYRO3 sequence (reverse complement)

Forward primer 1: 5'-AATT (overhang) - G/AATTC (EcoR1 Recognition site)-ATGGGAGCCCCGGTGAAG (TYRO3 sequence)-3'

Forward primer 2: 5'- AATT (overhang) - G/AATTC (EcoR1 Recognition site)-ATGGAGGAGCCTGACATC (TYRO3 sequence)- 3'

Figure 5. EcoRI restriction enzyme cut site, NEB #R3101.

Reverse primer: 5'- Myc fused with vector– TCGA (overhang) – C/TCGAG (Xho1 recognition site) - ACAGCTACTGTGTGGCAG (TYRO3 reverse complement sequence)-3'

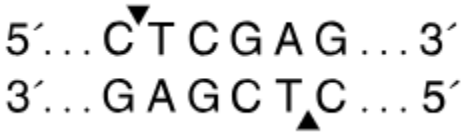

Figure 6. XhoI restriction enzyme cut site, NEB #R0146.

Forward primer Tm= 4(12)+2(6)= 60 C or Tm= 69,3+(0,41 x 66,7%) –(650/18)= 60,53 C

Reverse primer Tm= 4(10)+2(8)= 56 C or Tm=69,3+(0,41 x 55,6%) –(650/18)= 55,98 C

4.3. Molecular cloning of the TYRO3 Isoforms 1 and 2

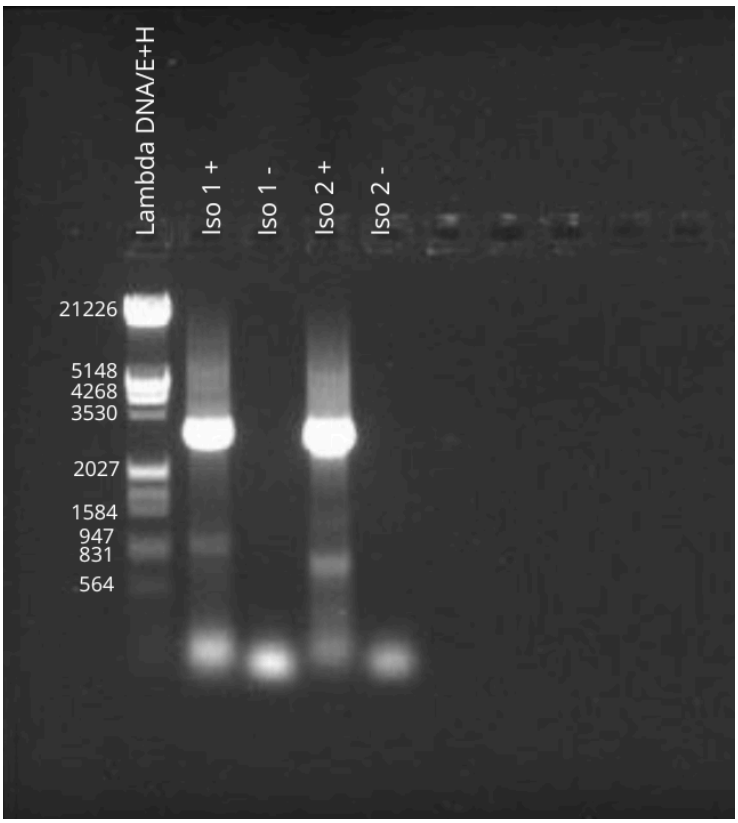

Figure 7. PCR amplification of TYRO3 Isoform 1 and 2. Wells: 1- Lambda DNA/E+H, 2- PCR product with Isoform 1, 3- Isoform 1 negative control, 4- PCR product with Isoform 2, 5- Isoform 2 negative control. Exposure 1 sec.

PCR amplification was set following the protocol outlined in the methods section. The outcomes are shown in Figure 7. Supercoiled and open circular conformation of TYRO3 Isoforms are depicted. Open circular (oc) DNA of TYRO3 Isoform 1 and 2 within the 3530 to 2027 bp range. Whereas compact supercoiled (ccc) DNA runs faster through the gel and is shown at 940 bp for Isoform 1 and at 830 for Isoform 2. A negative control was included to confirm the absence of PCR reagents contamination.

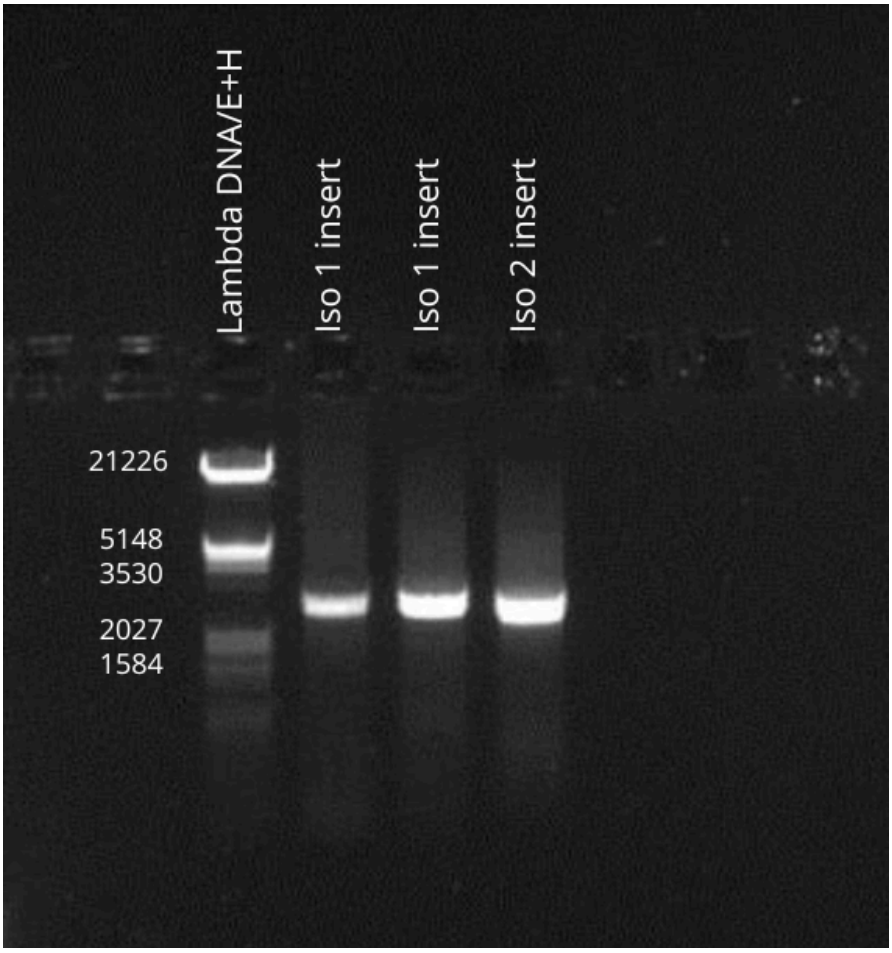

Figure 8. Purified PCR products. Wells:1 - lambda DNA/E+H, 2 - purified PCR product Iso 1, 3- purified PCR product Iso 1, 4- purified PCR product Iso 2.

PCR products purification was conducted following the protocol outlined in the methods section. Purified PCR products and DNA marker depicted in Figure 8.

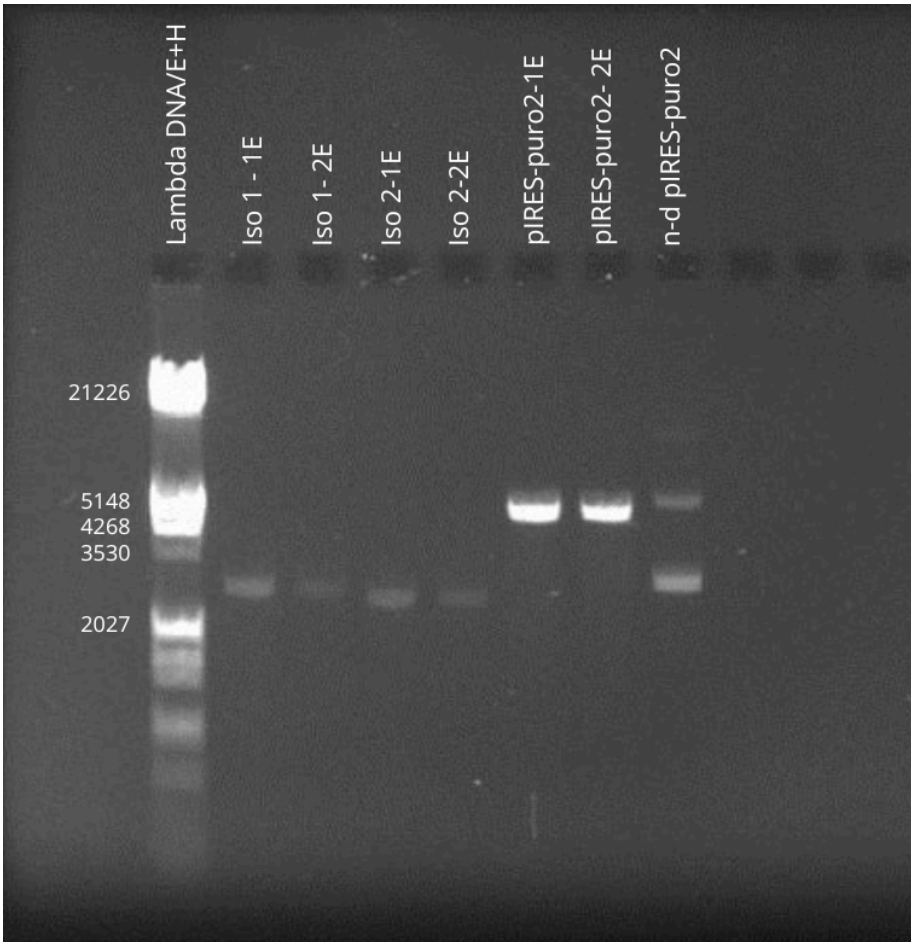

Figure 9. Digested and purified elutions of pIRES-puro2 (vector), TYRO3 Isoform 1 and 2 (insert). Wells: 1- Lambda DNA/E+H, 2- Iso-1 1 elution, 3- Iso-1 2 elution, 4- Iso-2 1 elution, 5- Iso-2 2 elution, 6- pIRES-puro2 1 elution, 7- pIRES-puro2 2 elution, 8- Undigested pIRES-puro2.

pIRES-puro2, TYRO3 Isoform 1 and 2 was cut with EcoRI and NheI restriction enzymes and purified afterwards. Figure 9 shows the TYRO3 Isoform 1 and 2 inserts are located between the 3530 to 2027 bp range, roughly at 2700 bp. Two elution fractions were done upon purification. The bands are not bright, which suggests that additional purification may decrease the concentration of inserts. The vector- pIRES-puro2 is located at 4900 bp and has a strong signal indicating a high concentration. Undigested vector has two bands, depicting oc and ccc confirmation at 5100-5148 and 2800-3000 bp, respectively.

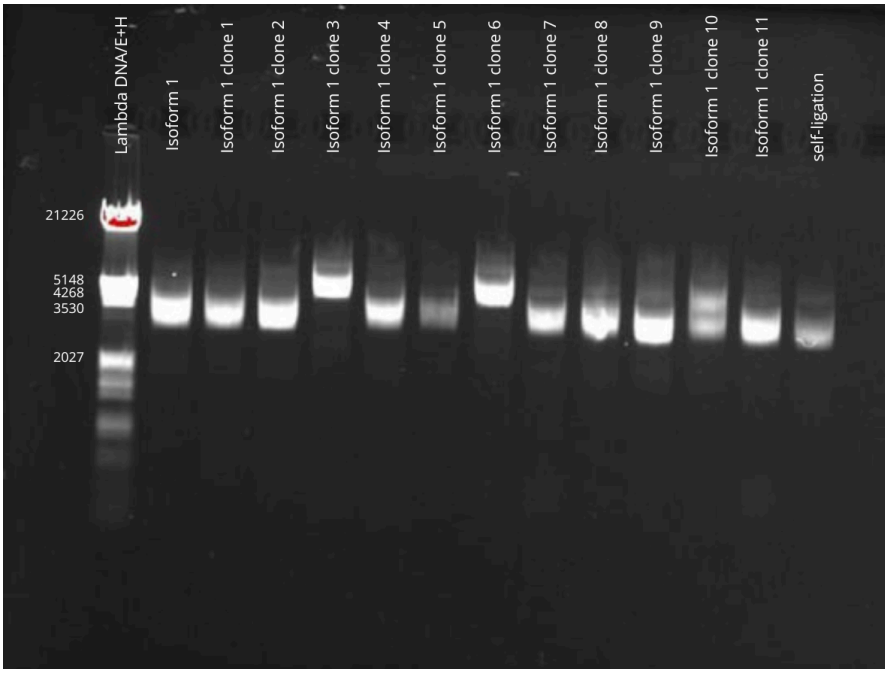

Figure 10. Plasmid isolation the following day from overnight cultures of Isoform 1. Wells: 1- lambda DNA/E+H, 2-13 Isoform 1 clones, 14- self-ligated vector

Ligation (Vector DNA 100 ng/µl, 1 µl and Insert 17 ng/µl, 2 µl) and transformation were completed. Distinct colonies (XL-1 blue) from the plate were selected for overnight culture, and plasmids isolations were performed. A plasmid prepared from the culture of bacteria transformed with a self-ligated vector was included as a negative control. Figure 10 shows Isoform 1 clones 4 and 7 differ in size from the self-ligated vector; therefore, they are considered successful clones of TYRO3 Isoform 1.

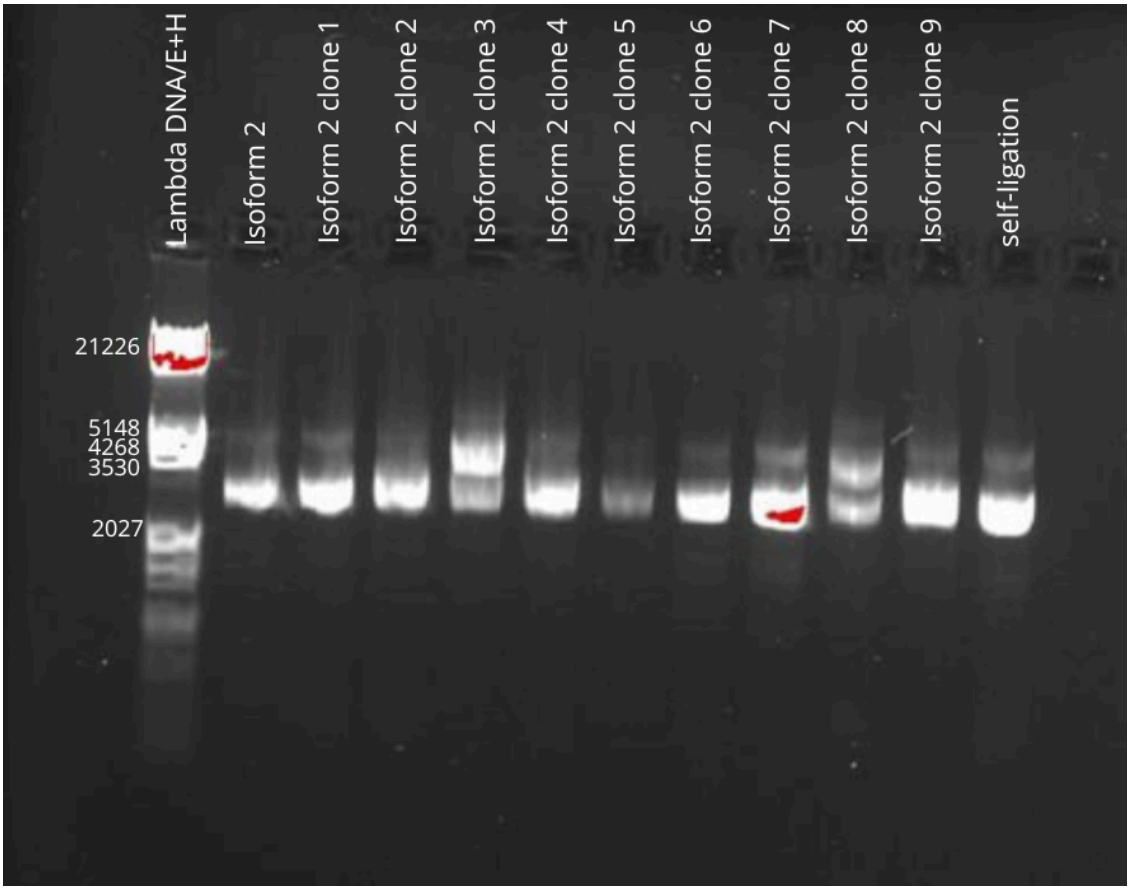

Figure 11. Plasmid isolation from overnight cultures of Isoform 2. Wells: 1- lambda DNA/E+H, 2-11 Isoform 1 clones, 12- self-ligated vector

Figure 11 indicates that no plasmid of Isoform 2 was isolated from the overnight culture. All the plasmid isolations matched the size of the negative control.

For TYRO3 Isoform 2, the repeat of the PCR amplification, digestion, ligation and transformation was done. This time, DHL5a competents cells were used for transformation, resulting in bigger colonies than in XL-1 blue cells. Colony screening PCR was performed.

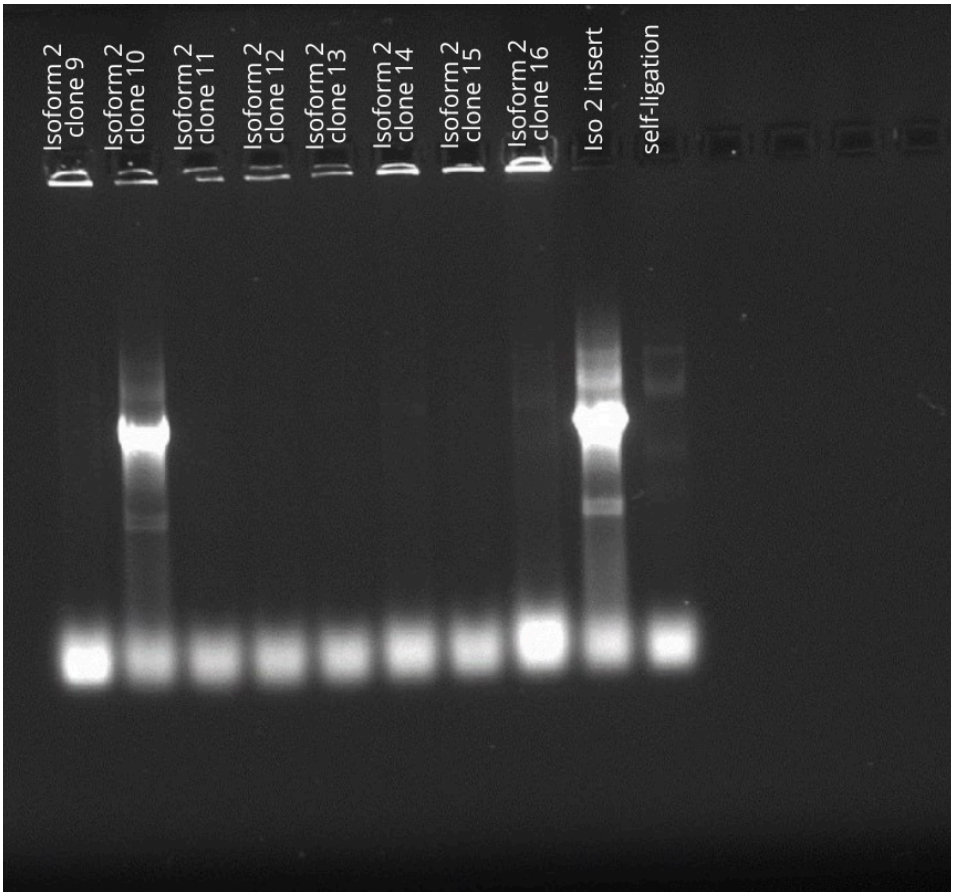

Figure 12. Colony PCR of Isoform 2 after transformation. Wells: 1-8 Isoform 2 clones, 9- Isoform 2 insert, 10- self-ligated vector

Clone 10 of Isoform 2 (Figure 12, second well on the gel) is the same size as the positive control- Isoform 2 insert. As a result, this specific clone has been selected for overnight culture for growing. Out of the 16 colonies, only one indicated an increase in size and were selected for further analysis.

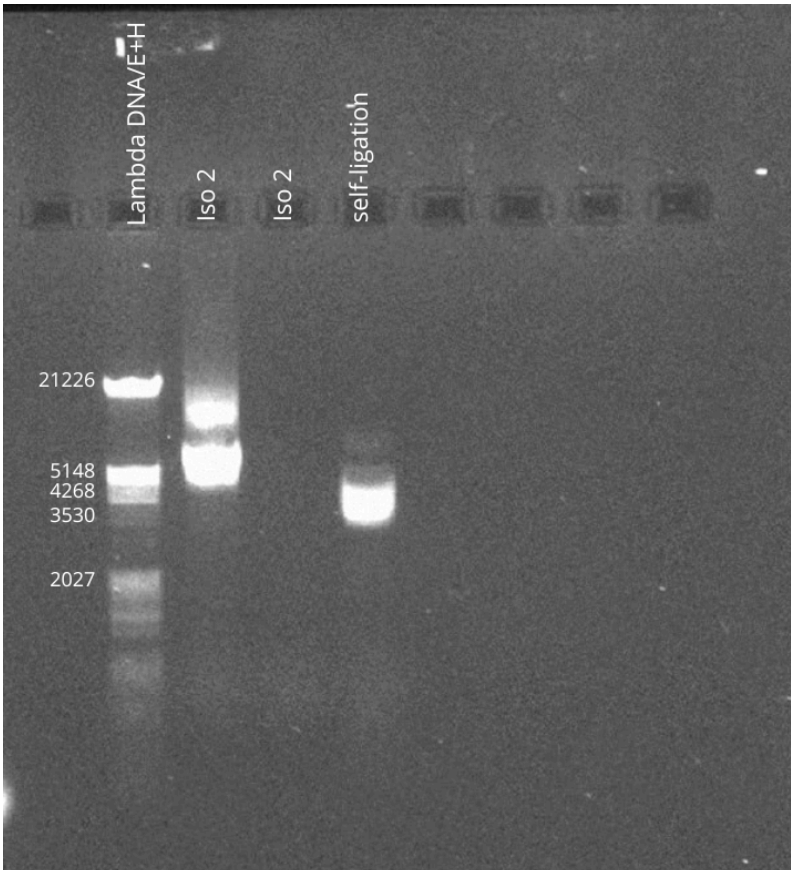

Figure 13. Plasmid isolation of Isoform 2 from overnight culture. Wells: 1-lambda DNA/E+H, 2 and 3- Iso 2, 4- self-ligated vector

Figure 13 shows that Isoform 2 clone 10 is located higher than the negative control (self-ligated vector) and has two bands because plasmid has super coiled(ccc) and open circular (oc) confirmations.

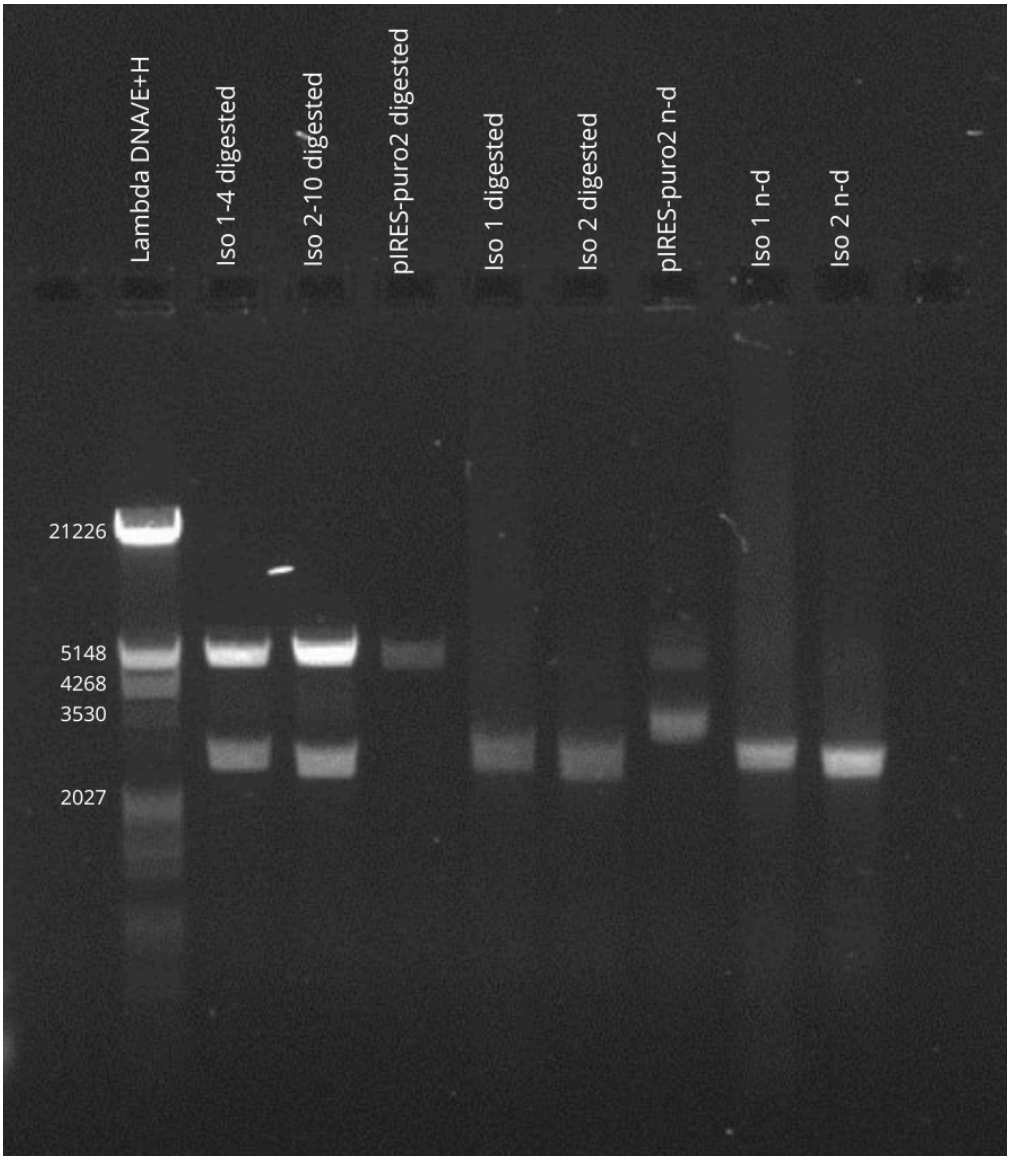

Figure 14. Image of digested TYRO3 Isoforms 1 and 2 with EcoRI and NheI and control plasmids. Wells: 1- Lambda DNA, 2- Iso 1-4 digested E+N, 3- Iso 2-10 digested E+N, 4- pIRES-puro2 vector digested E+N, 5- Iso 1 insert digested E+N, 6- Iso 2 insert digested E+N, 7- pIRES-puro2 vector undigested, 8- Iso 1 undigested, 9- Iso 2 undigested.

Figure 14 depicts the digestion of the TYRO3 Isoform 1 and 2 with EcoRI and NheI restriction enzymes. Cloning was successful as both isoforms exhibited bands similar to those of the vector and respective insert after digestion.

Each clone has two bands: higher position- pIRES-puro2 vector at 5100 bp, lower position - Isoform 1 insert at 2800 bp and Isoform 2 insert at 2700 bp.

After that, Isoforms 1 and 2 plasmid were isolated on MaxiPrep.

4.4. Transfection

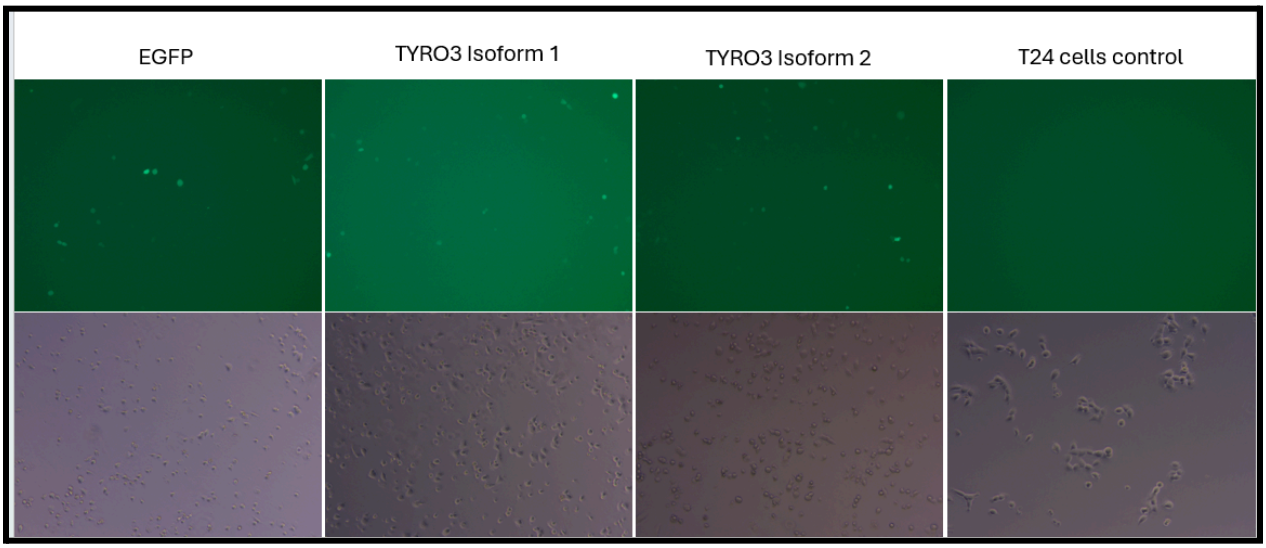

Figure 15. Transfection of T24 cell line with GFP and TYRO3 Isoforms 1 and 2 mix, non-transfected control cells on a 12 well-plate. Plasmids analyzed by ZEISS Primovert inverted microscope 24 hours post-transfection.

T24 cells were transfected with pEGFP plasmid, and co-transfections of TYRO3 Isoforms 1 and 2 with pEGFP plasmid (ratio 1:4) in order to control the efficiency of transfection were carried out using Lipofectamine 3000 as per the protocol described in the Methods section. Co-transfection with pEGFP is made to control transfection efficiency, as TYRO3 Isoforms do not have fluorescent tags. A 12-well plate was used, with 2 µl of Lipofectamine 3000 per well. The amount of TYRO3 Isoform 1 and 2 used was 1 µg each, while pEGFP in the control group was 1 µg, and in the co-transfected GFP group, it was 0.25 µg. The transfection efficiency, indicated by the green signal, was approximately 20%.

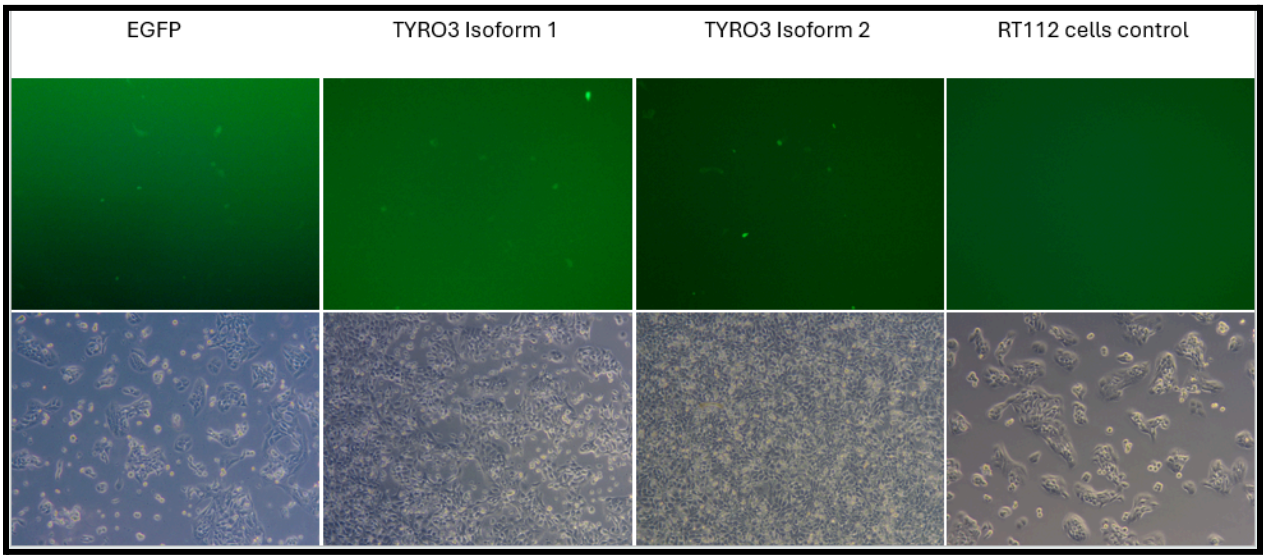

Figure 16. Transfection of RT112 cell line with GFP and TYRO3 Isoforms 1 and 2 mix, non-transfected control cells on a 12 well-plate. Transfected cells analyzed by ZEISS Primovert inverted microscope 24 hours post-transfection.

RT112 cells were transfected with GFP, and co-transfections of TYRO3 Isoforms 1 and 2 with GFP were carried out using Lipofectamine 3000 as protocol described in the Methods section. The same amounts of reagents were used as for the T24 cell line. Despite the cells reaching high confluency, the transfection efficiency was low at around 10% (Figure 16). The RT112 cell line may exhibit a lower efficiency in uptaking the plasmid compared to the T24 cell line.

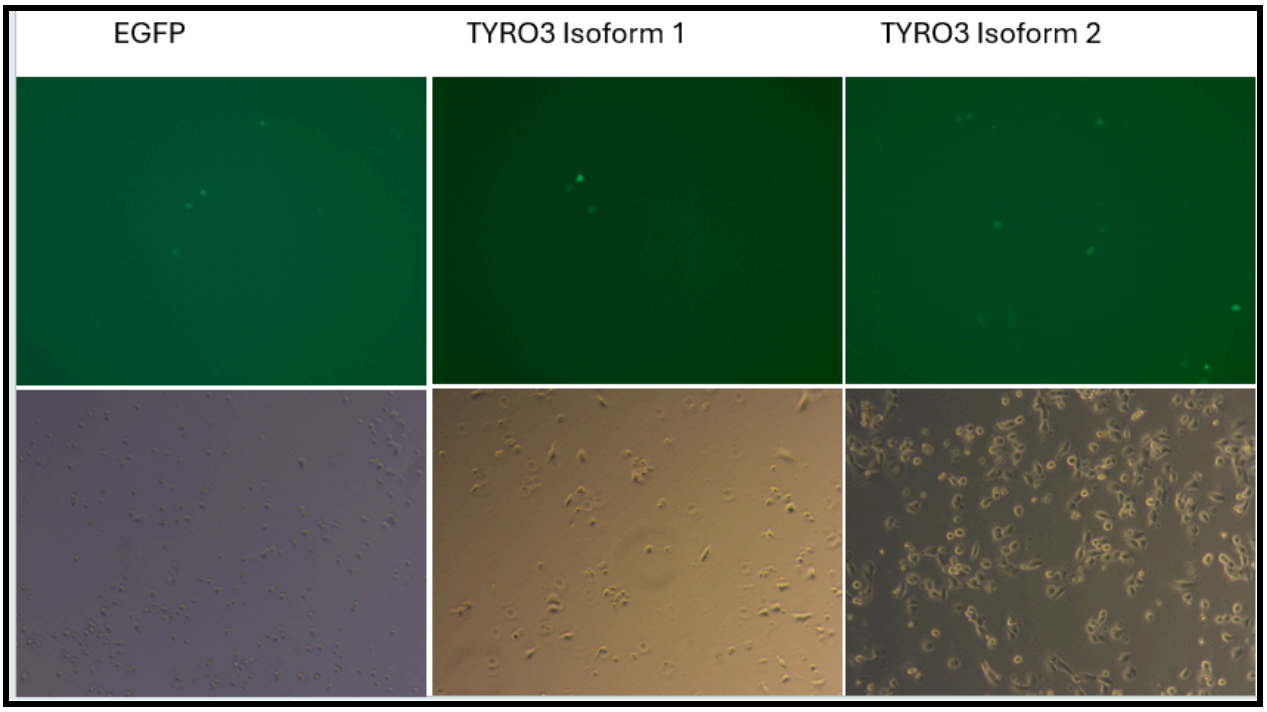

Figure 17. Transfection of T24 cell line with GFP/TYRO3 Isoforms 1 and 2 on a 6 well plate. Plasmids analyzed by ZEISS Primovert inverted microscope 48 hours post-transfection.

Figure 17 illustrates a significant decrease in T24 cell confluency after 24 hours of transfection with TYRO3 Isoform 1 and 2 plasmids using Lipofectamine 3000, followed by a 24-hour incubation period. This time, the volume of Lipofectamine 3000 used was 4.8 µl per well, with TYRO3 Isoform 1 and 2 amounts set at 2.5 µg. Consequently, only a minimal amount of transfected GFP plasmid can be observed. Upon transfection completion, 6 well-plate were used to make lysates.

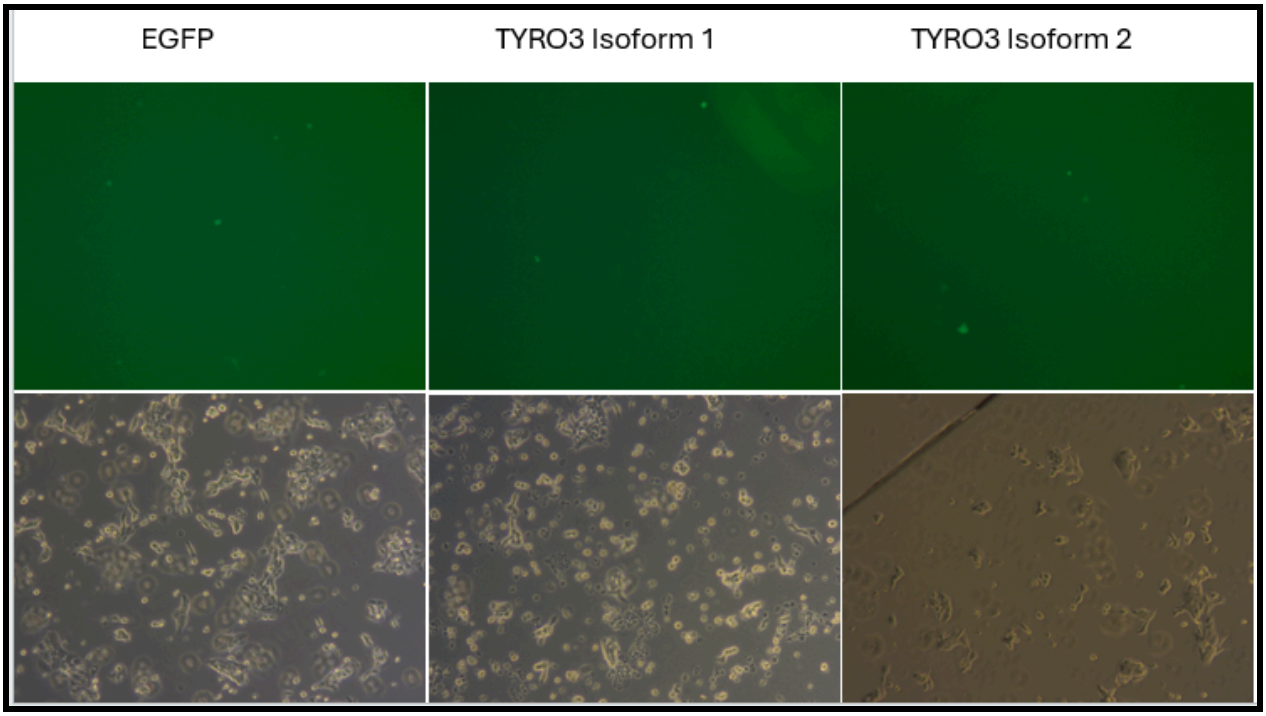

Figure 18. Transfection of RT112 cell line with GFP/TYRO3 Isoforms 1 and 2 on a 6 well plate. Plasmids analyzed by ZEISS Primovert inverted microscope 48 hours post-transfection.

Figure 18 illustrates the RT112 cell line transfected with TYRO3 Isoforms alongside with GFP plasmid. As noted before, the transfection rate decreased significantly with the chosen protocol, indicating a need for optimization. Upon transfection completion, lysates were prepared.

4.5. Western blot analysis

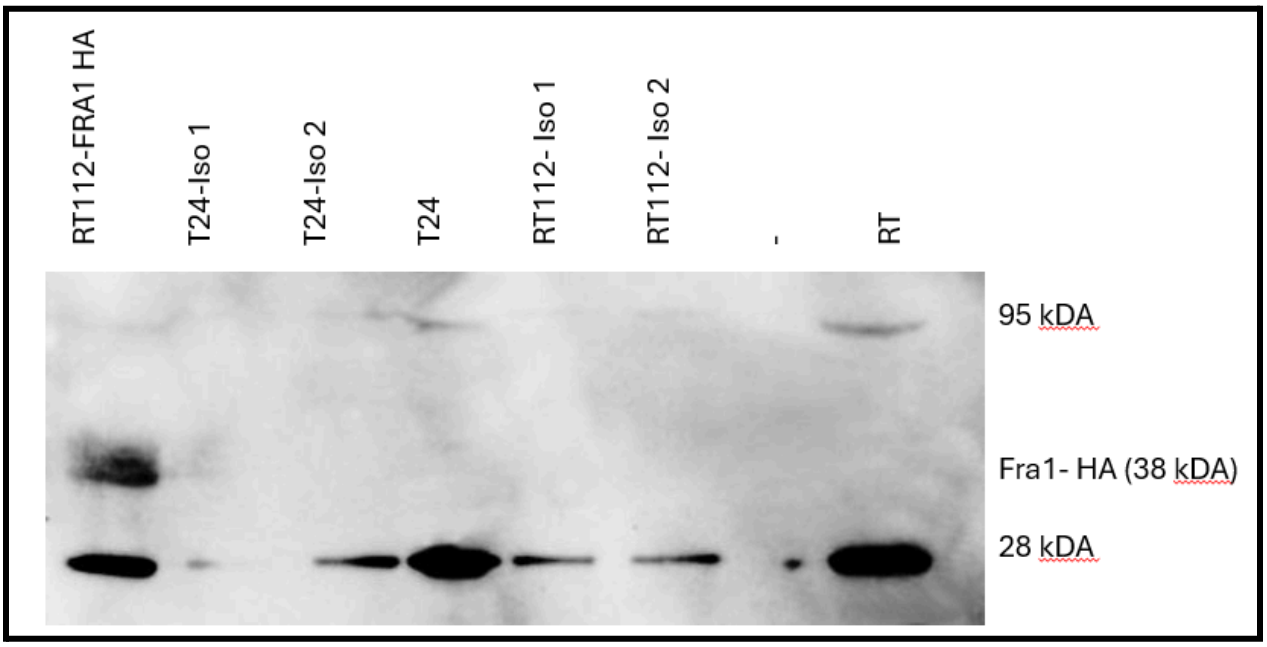

Figure 19. Expression of HA fusion proteins in the lysates of T24 and RT112 cells transfected with clones of TYRO3 Isoforms 1 and 2. Lysates of RT112 cells expressing HA-Fra1 protein were used as a positive control.

In Figure 19 the presence of the FRA1-HA fused protein on the RT112-FRA1 cell lines is seen on 38 kDA and is a positive control. According to Figure 19, the anti-HA antibody was not specific as other signals were found on the 28 kDa. Expected bands should have been located at 90-130 kDA on T24 and RT112 transfected cells with TYRO3 Isoform 1 and 2. There is a signal on the 95 kDA present in T24 and RT112 which is also non-specific.

Possible reason is high concentration of primary HA antibody and low concentration of TYRO3 Isoforms 1 and 2 in transfected cells.

5. DISCUSSION

5.1. Sequencing

Sanger sequencing has been used to confirm the actual nucleotide sequence of the insert that has been cloned into the vector. This method involves the annealing of amplified DNA fragments to an oligonucleotide primer. Subsequently, the DNA polymerase enzyme facilitates the extension by incorporating either a mixture of the four deoxynucleotide triphosphates or chain-terminating dideoxynucleotide triphosphates. The inclusion of these structures stops the DNA from further elongation, creating DNA fragments of varying lengths, thus enabling sequence analysis (Crossley et al, 2020). The Sanger sequencing was performed in accordance with the protocol described in the methods section.

Sequencing with 4 forward and one reverse primers from Table 3 were done. According to acquired data, clone of TYRO3 Isoform 1 with TYRO seq 1 primer had 99% query coverage and 98.99% identity with Homo sapiens TYRO3 protein tyrosine kinase, transcript variant 1 (Isoform 1), mRNA. While with TYRO seq 2 primer, it had 99% query coverage and 96.10% identity. Sequencing with TYRO seq 3 primer had 99% query coverage and 97.05% identity. TYRO seq 4 primer had less similarity covering 37% of the query and being 94.82% identical to the TYRO3 Isoform 1. TYRO rev seq primer had 53% of query cover and 98.54% identity, implying the problems with the obtaining of qualitative data.

Clone of TYRO3 Isoform 2 with TYRO seq primer had 100% query cover, while having 98.86% identity with the Homo sapiens TYRO3 protein tyrosine kinase, transcript variant 2, mRNA. Sequencing with TYRO seq 2 primer had 99% query coverage and 98.77% identity, while with TYRO seq 3 primer query cover was 99% and identity with TYRO3 Isoform 2 was 97.24%. Qualitative results were challenging to obtain with TYRO seq 4 primer which had 44% coverage and 95.81% identity and for the TYRO rev seq primer because it had no TYRO3 Isoform 2 sequence matched, mostly displaying cloning vectors.

It is suggested that Genetic DNA Analyzer had problems obtaining qualitative results while performing sequencing for TYRO3 Isoform 1 and 2 inserts with TYRO seq 4 and TYRO rev seq primers, as they were performed on the same day. Sequencing of recombinant plasmids should be repeated at another facility. Before final interpretation of the chromatogram, inspection of each strand with manual editing has been and should be done to check for the

artifacts, background noise, double and distorted peaks. The beginning and end of the sequence were cut off in order to have a clear nucleotide sequence, which is also advised when repeating the sequencing. Recommendation for further studies is to purify the DNA by various existing methods or improve DNA precipitation protocol before sending it to a sequencing analyzer. Crossley et al. (2020) suggest purification methods including bead-based, column-based, and enzymatic techniques. Furthermore, it is recommended to conduct gel electrophoresis with a DNA ladder to confirm the size of the sample before proceeding with sequencing.

5.2. Transfection protocol optimization

In the results part the issue of/with low transfection efficiency was described which also affected further analysis on Western blotting and immunofluorescence. Transfection protocol can be optimized the following ways:

Lipofectamine 3000 volume can vary between 3.75 to 7.5 ul, according to manufacturer instructions. Therefore, small volumes as 3.75 ul of the lipofectamine are advised for transfection with TYRO3 Isoforms 1 and 2 in a 6 well-plate. According to Figure 17 and Figure 18, T24 and RT112 cell lines confluency is decreased compared to Figure 15 and Figure 16. The higher concentration of used TYRO3 Isoform 1 and 2 might be toxic to the cells leading to cell death. Thus, the DNA amount should be also decreased to 1.5-1.75 ug. High amounts such as 2.5 ug led to low transfection efficiency confirmed by Western Blotting in Figure 19. According to obtained data, Isoform 2 seems to be less toxic than Isoform 1 to the T24 and RT112 cell lines, leading to higher transfection rates.

Other methods such as electroporation can be used to transfect T24 and RT112 cells with TYRO3 Isoforms. Electroporation, which uses high-voltage electric shocks to transport DNA into cells, is compatible with a variety of cell types. It causes a high rate of both long-term and transient gene expression. Furthermore, because of its simplified procedure, it might be more straightforward than other transfection methods (Potter, H., & Heller, R., 2018).

.

Some optimized parameters of the electroporation protocol can be used to get high transfection efficiency. Gehl (2003) suggests taking into account the cell size because it is inversely correlated with the external field responsible for permeabilization. Thus, T24 cells with the homogenic cell morphology could have higher transfection rates via this method. Furthermore, temperature manipulation might be recommended since temperature decrease during permeabilization with following heating elevates transfection rates and cell viability.

5.3. Western Blotting optimization

As mentioned before Western blotting results were not specific. In order to get positive results, transfection protocol should be optimized and cell confluency should be high >80% when preparing lysates for WB. Recommendation for further studies is to purchase and use another HA antibody which will be more specific.

Another suggestion is to use anti-myc antibody because it is high specificity to Myc epitope. Therefore, new primers with the myc tag sequence should be used. The primer design using myc tag was presented at the Results section and could be promptly used for further studies. This study used HA tag because it was delivered and was ready to start with the PCR amplification.

Analysis of TYRO3 localization by Immunofluorescence was not done in this project because the results of the WB did not confirm the presence of the protein of interest and demanded more time in a laboratory than was specified by the program. The Immunofluorescence analysis was not specific, displaying mainly artifacts and non-specific proteins in T24 and RT112 transfected cells. The IF of positive control RT112-FRA1-HA tag was done and is present on the Appendix. The clear edges of the attached cells seen and FRA1-HA fusion protein present on the cytoplasm being colored with GFP and nucleus with DAPI.

6. Conclusion

Understanding the localization of TYRO3 Isoform 2 could reveal its potential involvement in the gene expression of TYRO3, an important protein in bladder cancer cells. Additional research with recommendations outlined here could uncover novel insights into TYRO3 and bladder cancer, leading to the development of new cancer treatment options.

7. Appendix

Sequencing analysis

Iso-1 TYRO seq 1 chromatogram:

AAACCGAGATCTCCCAGCCAGTGTGGCTAGGAAGAAGGtGTGCCATTTTTCACAGTG
GAGCCAAAAGATCTGGCAGTGCCACCCAATGCCCCTTTCCAACTGTCTTGTGAGGCT
GTGGGTCCCCCTGAACCTGTTACCATTGTCTGGTGGAGAGGAACTACGAAGATCGGG
GGACCCGCTCCCTCTCCATCTGTTTTAAATGTAACAGGGGTGACCCAGAGCACCATGT
TTTCCTGTGAAGCTCACAACCTAAAAGGCCTGGCCTCTTCTCGCACAGCCACTGTTC
ACCTTCAAGCACTGCCTGCAGCCCCCTTCAACATCACCGTGACAAAGCTTTCCAGCA
GCAACGCTAGTGTGGCCTGGATGCCAGGTGCCGATGGCCGAGCTCTGCTACAGTCCT
GTACAGTTCTKGTGACACAGGCCCCAGGAGGCTGGGAAGTCCTGGCTGTTGTGGTCC
CTGTGCCCCCCTTTACCTGCCTGCTCCGGGACCTGGTGCATGCCACCAACTACAGCCT
CAGGGTGCGCTGTGCCAATGCCTTGGGGCCCTCTCCCTAGGCTGACTGGGTGCCCTTT
CAGACCAAGGGTCTAGCCCCAGCCAGCGCTCCCCAAAACCTCCATGCCATCCGCACA
GATTCAGGCCTCATCTTGGAGTGGGAAGAAGTGATCCCCGAGGCCCCTTTGGAAGGC
CCCCC

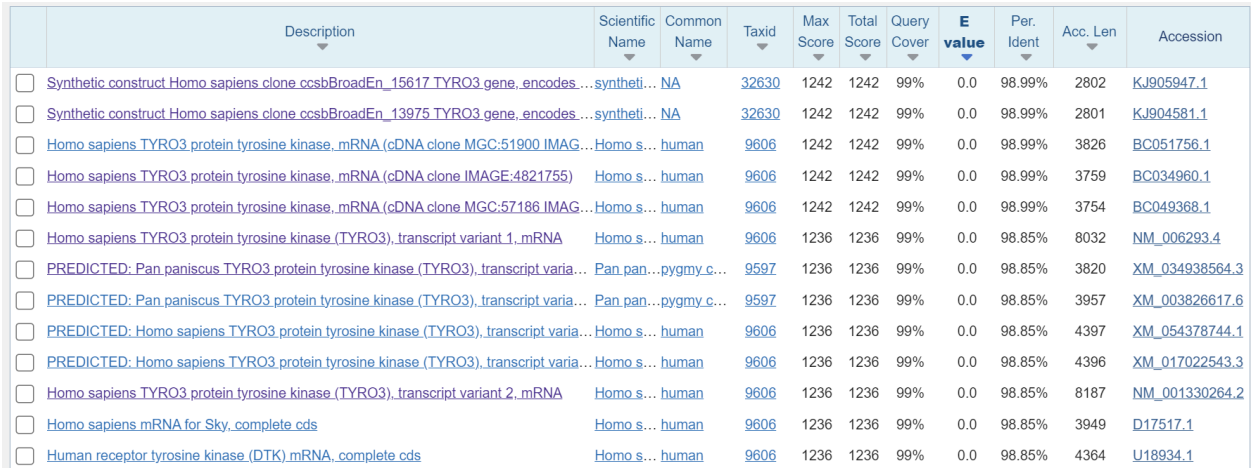

Description	Scientific Name	Common Name	Taxid	Max Score	Total Score	Query Cover	E value	Per. Ident	Acc. Len	Accession
Synthetic construct Homo sapiens clone ccsbBroadEn_15617 TYRO3 gene, encodes …	syntheti…	NA	32630	1242	1242	99%	0.0	98.99%	2802	KJ905947.1
Synthetic construct Homo sapiens clone ccsbBroadEn_13975 TYRO3 gene, encodes …	syntheti…	NA	32630	1242	1242	99%	0.0	98.99%	2801	KJ904581.1
Homo sapiens TYRO3 protein tyrosine kinase, mRNA (cDNA clone MGC:51900 IMAG…	Homo s…	human	9606	1242	1242	99%	0.0	98.99%	3826	BC051756.1
Homo sapiens TYRO3 protein tyrosine kinase, mRNA (cDNA clone IMAGE:4821755)	Homo s…	human	9606	1242	1242	99%	0.0	98.99%	3759	BC034960.1
Homo sapiens TYRO3 protein tyrosine kinase, mRNA (cDNA clone MGC:57186 IMAG…	Homo s…	human	9606	1242	1242	99%	0.0	98.99%	3754	BC049368.1
Homo sapiens TYRO3 protein tyrosine kinase (TYRO3), transcript variant 1, mRNA	Homo s…	human	9606	1236	1236	99%	0.0	98.85%	8032	NM_006293.4
PREDICTED: Pan paniscus TYRO3 protein tyrosine kinase (TYRO3), transcript varia…	Pan pan…	pygmy c…	9597	1236	1236	99%	0.0	98.85%	3820	XM_034938564.3
PREDICTED: Pan paniscus TYRO3 protein tyrosine kinase (TYRO3), transcript varia…	Pan pan…	pygmy c…	9597	1236	1236	99%	0.0	98.85%	3957	XM_003826617.6
PREDICTED: Homo sapiens TYRO3 protein tyrosine kinase (TYRO3), transcript varia…	Homo s…	human	9606	1236	1236	99%	0.0	98.85%	4397	XM_054378744.1
PREDICTED: Homo sapiens TYRO3 protein tyrosine kinase (TYRO3), transcript varia…	Homo s…	human	9606	1236	1236	99%	0.0	98.85%	4396	XM_017022543.3
Homo sapiens TYRO3 protein tyrosine kinase (TYRO3), transcript variant 2, mRNA	Homo s…	human	9606	1236	1236	99%	0.0	98.85%	8187	NM_001330264.2
Homo sapiens mRNA for Sky, complete cds	Homo s…	human	9606	1236	1236	99%	0.0	98.85%	3949	D17517.1
Human receptor tyrosine kinase (DTK) mRNA, complete cds	Homo s…	human	9606	1236	1236	99%	0.0	98.85%	4364	U18934.1

Figure 20. BLAST analysis of Iso-1 TYRO seq 1

Iso -1 with TYRO3 seq 2 chromatogram

CTGGGTTCAAGACAATGGAAAAAGGCGGAGCTGACAGTGGAGGGGACCAGGGCCA
ATCCGACAGGCTGGGATCCCCAAAAGGACCTGATCGTACGTGTGTGCGTCTCCAATG
CAGTTGGCTGTGGACCCTGGAGTCAGCCACTGGTGGTCTCTTCTCATGACCGTGCAG
GCCAGCAGGGCCCTCCTCACAGCCGCACATCCTGGGTACCTGTGGTCCTTGGTGTGC
TAACGGCCCTGGTGACGGCTGCTGCCCTGGCCCTCATCCTGCTTCGAAAGAGACGGA
AAGAGACGCGGTTTGGGCAAGCCTTTGACAGTGTCATGGCCCGGGGAGAGCCAGCC
GTTCACTTCCGGGCAGCCCGGTCCTTCAATCGAGAAAGGCCCGAGCGCATCGAGGCC
ACTTTGKACAGCTTGGGCATCAGCGATGAACTAAAGGAAAAACTGGAGGATGTGCTC
ATCCCAGAGCAGCAGTTCACCCTGGGCCGGATGTTGGGCAAAGGAGAGTTTGGTTCA
GTGCGGGAGGCCCAGCTGAAGCAAGAGGATAGCTCCTTTGTGAAAGTGGCTGTGAA
GATGCTGAAAGCTGACATCATTGCCTCAAGCGACATTGAAGAGTTCCTCAGGGAAGC
AGCTTGCATGAAGGAGTTTGACCATCCACACGTGGCCAAACTTGTTGGGGGTAAGCC
TCCGGAGCAGGGCTAAGGGCCGTCTCCCCCATCCCCATGGTCATCTTGCCCTTTCATG
AAGCATGGGGACCTGCATGCCTTTCCTGCTCcGCCTCCcCGGGATTGGGGAGAACCCC
TTTAACCCTACCCCTCCAGAACCCTgGATCCGGTTTCATGGTGGACATTGCCTGCGCAT
GGAGTACCTGGAGCTCTTCGAAACCTTCATTCCcACCGGAGaAACCTGGACCTGCCTC
GGAAATTGGCC

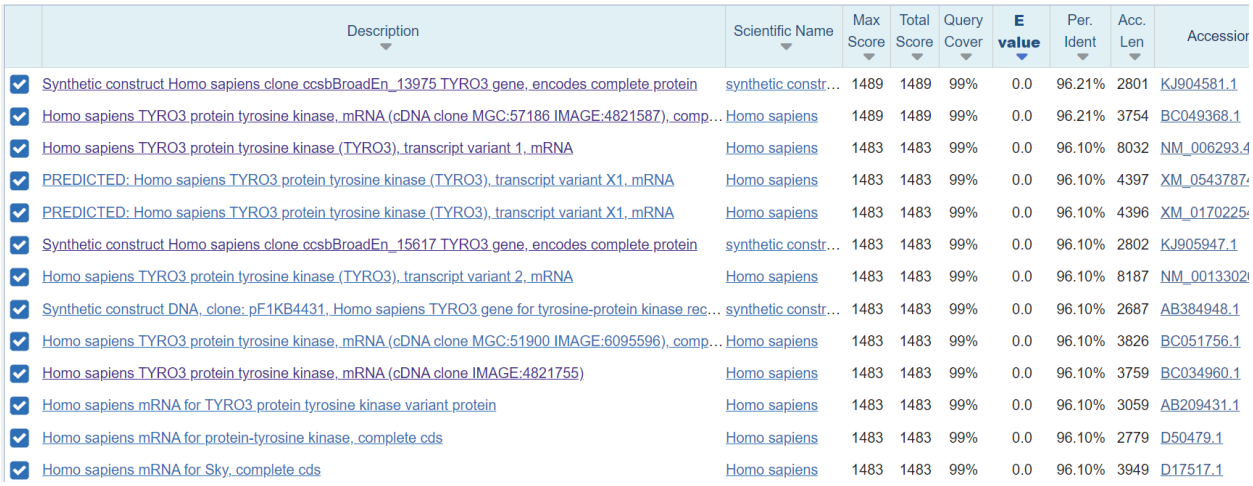

Description	Scientific Name	Max Score	Total Score	Query Cover	E value	Per. Ident	Acc. Len	Accession
Synthetic construct Homo sapiens clone ccsbBroadEn_13975 TYRO3 gene, encodes complete protein	synthetic constr…	1489	1489	99%	0.0	96.21%	2801	KJ904581.1
Homo sapiens TYRO3 protein tyrosine kinase, mRNA (cDNA clone MGC:57186 IMAGE:4821587), comp…	Homo sapiens	1489	1489	99%	0.0	96.21%	3754	BC049368.1
Homo sapiens TYRO3 protein tyrosine kinase (TYRO3), transcript variant 1, mRNA	Homo sapiens	1483	1483	99%	0.0	96.10%	8032	NM_006293.4
PREDICTED: Homo sapiens TYRO3 protein tyrosine kinase (TYRO3), transcript variant X1, mRNA	Homo sapiens	1483	1483	99%	0.0	96.10%	4397	XM_0543787
PREDICTED: Homo sapiens TYRO3 protein tyrosine kinase (TYRO3), transcript variant X1, mRNA	Homo sapiens	1483	1483	99%	0.0	96.10%	4396	XM_0170225
Synthetic construct Homo sapiens clone ccsbBroadEn_15617 TYRO3 gene, encodes complete protein	synthetic constr…	1483	1483	99%	0.0	96.10%	2802	KJ905947.1
Homo sapiens TYRO3 protein tyrosine kinase (TYRO3), transcript variant 2, mRNA	Homo sapiens	1483	1483	99%	0.0	96.10%	8187	NM_0013302
Synthetic construct DNA, clone: pF1KB4431, Homo sapiens TYRO3 gene for tyrosine-protein kinase rec…	synthetic constr…	1483	1483	99%	0.0	96.10%	2687	AB384948.1
Homo sapiens TYRO3 protein tyrosine kinase, mRNA (cDNA clone MGC:51900 IMAGE:6095596), comp…	Homo sapiens	1483	1483	99%	0.0	96.10%	3826	BC051756.1
Homo sapiens TYRO3 protein tyrosine kinase, mRNA (cDNA clone IMAGE:4821755)	Homo sapiens	1483	1483	99%	0.0	96.10%	3759	BC034960.1
Homo sapiens mRNA for TYRO3 protein tyrosine kinase variant protein	Homo sapiens	1483	1483	99%	0.0	96.10%	3059	AB209431.1
Homo sapiens mRNA for protein-tyrosine kinase, complete cds	Homo sapiens	1483	1483	99%	0.0	96.10%	2779	D50479.1
Homo sapiens mRNA for Sky, complete cds	Homo sapiens	1483	1483	99%	0.0	96.10%	3949	D17517.1

Figure 21. BLAST analysis of Iso-1 TYRO seq 2

Iso-1 with Tyro seq 3 chromatogram

CWTGYCCAMTTGTTTGGGGGTAGCCTCCGGAGCAGGGCTAAAGGCCGTCTCCCCAT
CCCCATGGtCATCTGACCTAAATGAAGCATGGGGACCTGCATGCCTTCCTGCTCSCCTC
CCGGATTGGGGAGAACCCCTTTAACCTACCCCTCCAGACCCTGATCCGGTTCATGGTG
GACATTGCCTGCGGCATGGAGTACCTGAGCTCTCGGAACTTCATCCACCGAGACCTG
GCTGCTCGGAATTGCATGCTGGCAGAGGACATGACAGTGTGTGTGGCTGACTTCGGA
CTCTCCCGGAAGATCTACAGTGGGGACTACTATCGTCAAGGCTGTGCCTCCAAACTGC
CTGTCAAGTGGCTGGCCCTGGAGAGCCTGGCCGACAACCTGTATACTGTGCAGAGTG
ACGTGTGGGCGTTCGGGGTGACCATGTGGGAGATCATGACACGTGGGCAGACGCCAT
ATGCTGGCATCGAAAACGCTGAGATTTACAACTACCTCATTGGCGGGAACCGCCTGA
AACAGCCTCCGGAGTGTATGGAGGACGTGTATGATCTCATGTACCAGTGCTGGAGTGC
TGACCCCAAGCAGCGCCCGAGCTTTACTTGTCTGCGAATGGAACTGGAGAACATCTT
GGGCCAGCTGTCTGTGCTATCTGCCAGCCAGGACCCCTTATACATCAACATCGAGAGA
GCTGAGGAGCCCACTGCGGGAGGGCAGCATGGARCTACCTGGCGGGGGATCAGCCC
CTACAGTGGGGGCTGGGGGATGGGCAGTGGCCATGGGGGGGCAGTGGGTGGCACTC
CCCAGTGGACTGTCGGGTACATACTCCACCCCCCCGGAAGGGGCTGACTGGAGCAGC
CCAGGGACAGGMCAGAAGCACCCAGCCCAGGAAGAAGTTCCCCTCCAATGGAGAA
CMACCAGAAGGCTTTTTGGCTGCTGTCAGCAAGGCCCTAMCGGCCCCCMACRGTAA

GCTTGTTAATCCCATTATKGATGGTTTACAGGATAATGCTGGAATTCCGCGGAATYCCG
CGCGGGTGC

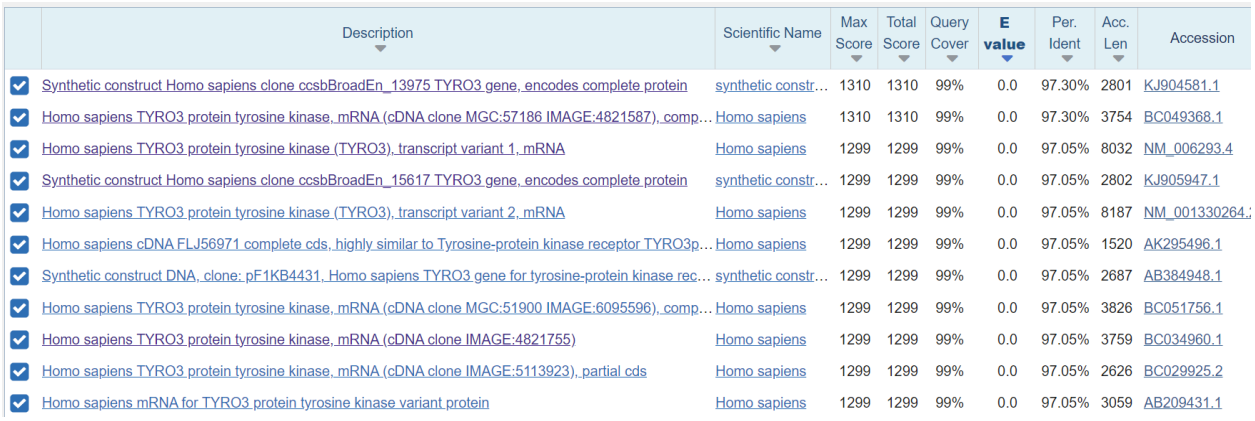

Description	Scientific Name	Max Score	Total Score	Query Cover	E value	Per. Ident	Acc. Len	Accession
Synthetic construct Homo sapiens clone ccsbBroadEn_13975 TYRO3 gene, encodes complete protein	synthetic constr…	1310	1310	99%	0.0	97.30%	2801	KJ904581.1
Homo sapiens TYRO3 protein tyrosine kinase, mRNA (cDNA clone MGC:57186 IMAGE:4821587), comp…	Homo sapiens	1310	1310	99%	0.0	97.30%	3754	BC049368.1
Homo sapiens TYRO3 protein tyrosine kinase (TYRO3), transcript variant 1, mRNA	Homo sapiens	1299	1299	99%	0.0	97.05%	8032	NM_006293.4
Synthetic construct Homo sapiens clone ccsbBroadEn_15617 TYRO3 gene, encodes complete protein	synthetic constr…	1299	1299	99%	0.0	97.05%	2802	KJ905947.1
Homo sapiens TYRO3 protein tyrosine kinase (TYRO3), transcript variant 2, mRNA	Homo sapiens	1299	1299	99%	0.0	97.05%	8187	NM_001330264.2
Homo sapiens cDNA FLJ56971 complete cds, highly similar to Tyrosine-protein kinase receptor TYRO3p…	Homo sapiens	1299	1299	99%	0.0	97.05%	1520	AK295496.1
Synthetic construct DNA, clone: pF1KB4431, Homo sapiens TYRO3 gene for tyrosine-protein kinase rec…	synthetic constr…	1299	1299	99%	0.0	97.05%	2687	AB384948.1
Homo sapiens TYRO3 protein tyrosine kinase, mRNA (cDNA clone MGC:51900 IMAGE:6095596), comp…	Homo sapiens	1299	1299	99%	0.0	97.05%	3826	BC051756.1
Homo sapiens TYRO3 protein tyrosine kinase, mRNA (cDNA clone IMAGE:4821755)	Homo sapiens	1299	1299	99%	0.0	97.05%	3759	BC034960.1
Homo sapiens TYRO3 protein tyrosine kinase, mRNA (cDNA clone IMAGE:5113923), partial cds	Homo sapiens	1299	1299	99%	0.0	97.05%	2626	BC029925.2
Homo sapiens mRNA for TYRO3 protein tyrosine kinase variant protein	Homo sapiens	1299	1299	99%	0.0	97.05%	3059	AB209431.1

Figure 22. BLAST analysis of Iso-1 TYRO seq 3

Iso 1 with TYRO seq 4 chromatogram

TGCGAATGGAACTGGAGAAAGGAAGGGGCGGGGTGTCTGTGCTATCTGCCAGCCAG
GACCCCCACACATAGAAATCGAGAGAGCTGAGGAGCCCACTGCGGGAGGCAGCATG
GAGCTACCTGGCGGGGATCAGCCCTACAGTGGGGCTGGGGATGGCAGTGGCATGGG
GGCAGTGGGTGGCACTCCCAGTGACTGTCGGTACATACTCACCCCCGGAGGGCTGGC
TGAGCAGCCAGGGCAGGCAGAGCACCAGCCAGAGAGTCCCCTCAATGAGACACAGA
GGCTTTTGCTGCTGCAGCAAGGGCTACTGCCACACAGTAGCTGTTATCCATATGATGT
TCCAGATTATGCTGAATTCGGATCCGCGGCCGCATAGATAACTGATCCAGTGTGCTGG
AATTAATTCTTTGTCTGTTAGGGCCAGCTGTTGGGGTGAGTACTCCCTCTCAAAAGCG
GGCATGACTTCTGCGCTAAGATTGTCAGTTTCCAAAAACGAGGAGGATTTGATATTCA
CCTGGCCCCGCGGTGATGCCTTTGAGGGGTGGCCGCCGTCCATCCTGGGTCAGAAAA
AGACAATCTTTTTTGTTGTCAAGCTTTGAAGGTGTGGGCAGGGCTTTGAGATCTTGGG
CCATACACTTTGAGTGGACAATGACAATCCACTTTTGCCTTTTCTCCTCCACAGGGGG
TCCCACTCCCAGGGTCCAACTTGCMAGGGTCCGAGCATGGCATCTAGGGGCGGCCCA
AWTTCCGGCCCCTTCTCCCCCCCCCCCCCCCCCTAAACGGTTAACCTGGGACCSAAA
GCCCGCTTTGGGAAAATAAGGGCCCGGTGGGGGCCGTTTGGTCTAATTATGGTTTATT
TTTCCCCACCC

Description	Scientific Name	Common Name	Taxid	Max Score	Total Score	Query Cover	E value	Per. Ident	Acc. Len	Accession
Synthetic construct Homo sapiens gateway clone IMAGE:100021050 3' read TYRO3 …	syntheti…	NA	32630	523	523	38%	3e-143	95.18%	1274	CU690613.1
Homo sapiens TYRO3 protein tyrosine kinase, mRNA (cDNA clone MGC:57186 IMAG…	Homo s…	human	9606	521	521	37%	1e-142	95.43%	3754	BC049368.1
Synthetic construct Homo sapiens clone ccsbBroadEn_13975 TYRO3 gene, encodes …	syntheti…	NA	32630	518	518	38%	1e-141	94.88%	2801	KJ904581.1
Cloning vector pTAP, complete sequence	Cloning …	NA	3031340	512	512	47%	7e-140	90.34%	5388	OP292672.1
Cloning vector pTAP-AFAP, complete sequence	Cloning …	NA	3031341	512	512	47%	7e-140	90.34%	6312	OP292671.1
Homo sapiens TYRO3 protein tyrosine kinase (TYRO3), transcript variant 1, mRNA	Homo s…	human	9606	510	510	37%	2e-139	94.82%	8032	NM_006293.4
Eukaryotic synthetic construct chromosome 15	eukaryo…	NA	111789	510	944	37%	2e-139	94.82%	82521392	CP034493.1
Homo sapiens chr13:43495695-43495691 non-reference unique insertion sequence	Homo s…	human	9606	510	510	37%	2e-139	94.82%	4961	MH533457.1
Homo sapiens isolate NA24385 chromosome 15	Homo s…	human	9606	510	944	37%	2e-139	94.82%	96257017	CP139551.1
Homo sapiens TYRO3 protein tyrosine kinase (TYRO3), RefSeqGene on chromosom…	Homo s…	human	9606	510	510	37%	2e-139	94.82%	31378	NG_033013.2
Homo sapiens isolate CHM13 chromosome 15	Homo s…	human	9606	510	944	37%	2e-139	94.82%	99753195	CP068263.2
Homo sapiens DNA, chromosome 15, nearly complete genome	Homo s…	human	9606	510	944	37%	2e-139	94.82%	95537968	AP023475.1
Homo sapiens TYRO3 protein tyrosine kinase (TYRO3), transcript variant 2, mRNA	Homo s…	human	9606	510	510	37%	2e-139	94.82%	8187	NM_001330264.2

Figure 23. BLAST analysis of Iso-1 TYRO seq 4

Iso 1 with TYRO rev seq

CACCTTCTACCGTGAGCCACACTGGGGgGAGATCTcGGTTTCACCCCCATCCTCCACC
TGGCACCAgTACCGGMCGGCGTCAGAGCGCTCCACTGACTTCAGGCTGAGGAAGCC
GATCCAGTGCTGCTCGCTGACTGGGATGTACAACTGGTCCAAGTTCTGGACCACAGC
CCCATCCTTCACCCACTGGATGTCAGGCTCCTCCATCCCCTCCACACTGCAGTTGAGC
TTCACCGGCTGCCCCTGAGACACTGTCAGCTTCACCGGGGCTCCCATGAGCTTCAGA
CCTGCGGCGGCGGACTCCGGGAGCAGCAGAGAAGCCAGAGCCGCCAGCAGCAGCC
CGAGCCGCAGTGGCGGCGGCAGCGGCAGCGGCTGGAGCCCCGGCCGCCCCATGCTC
CTCCTCAGCGCCATgcTagCTAGGCCGCAGATATCGATCCGAGCTCGGTACCAAGCTTG
GGTCTCCCTATAGTGAGTCGTATTAATTTCGATAAGCCAGTAAGCAGTGGGTTCTCTAG
TTAGCCAGAGAGCTCTGCTTATATAGACCTCCCACCGTACACGCCTACCGCCCATTTG
CGTCAATGGGGCGGAGTTGTTACGACATTTTGGAAAGTCCCGTTGATTTTGGTGCCAA
AACAAACTCCCATTGACGTCAATGGGGTGGAGACTTGGAAATCCCCGTGAGTCAAAC
CGCTATCCACGCCATTGATGTACTGCCAAAACCGCATCACCATGGGTAATAGCGATGA
CTAATACGTAaATGTACTGGCC

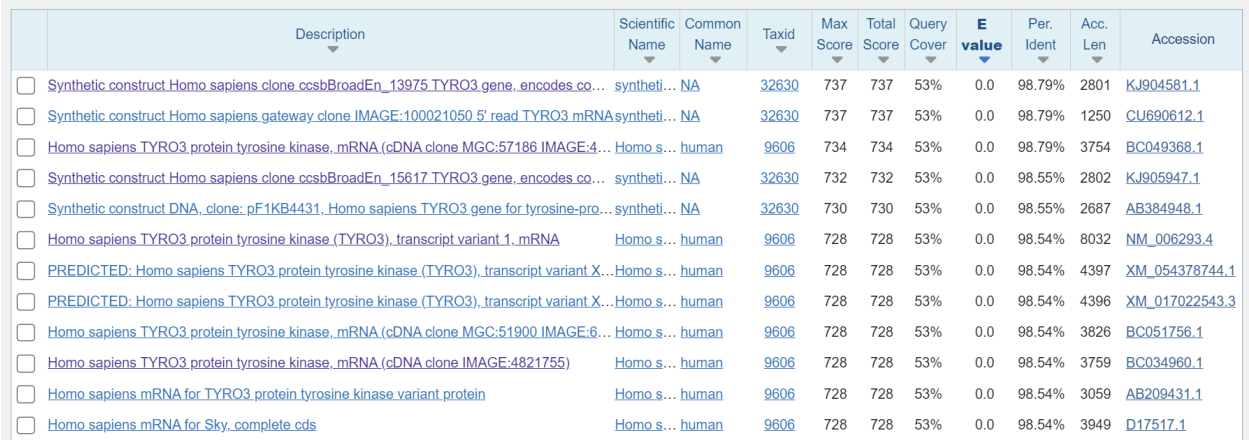

Description	Scientific Name	Common Name	Taxid	Max Score	Total Score	Query Cover	E value	Per. Ident	Acc. Len	Accession
Synthetic construct Homo sapiens clone ccsbBroadEn_13975 TYRO3 gene, encodes co…	syntheti…	NA	32630	737	737	53%	0.0	98.79%	2801	KJ904581.1
Synthetic construct Homo sapiens gateway clone IMAGE:100021050 5' read TYRO3 mRNA	syntheti…	NA	32630	737	737	53%	0.0	98.79%	1250	CU690612.1
Homo sapiens TYRO3 protein tyrosine kinase, mRNA (cDNA clone MGC:57186 IMAGE:4…	Homo s…	human	9606	734	734	53%	0.0	98.79%	3754	BC049368.1
Synthetic construct Homo sapiens clone ccsbBroadEn_15617 TYRO3 gene, encodes co…	syntheti…	NA	32630	732	732	53%	0.0	98.55%	2802	KJ905947.1
Synthetic construct DNA, clone: pF1KB4431, Homo sapiens TYRO3 gene for tyrosine-pro…	syntheti…	NA	32630	730	730	53%	0.0	98.55%	2687	AB384948.1
Homo sapiens TYRO3 protein tyrosine kinase (TYRO3), transcript variant 1, mRNA	Homo s…	human	9606	728	728	53%	0.0	98.54%	8032	NM_006293.4
PREDICTED: Homo sapiens TYRO3 protein tyrosine kinase (TYRO3), transcript variant X…	Homo s…	human	9606	728	728	53%	0.0	98.54%	4397	XM_054378744.1
PREDICTED: Homo sapiens TYRO3 protein tyrosine kinase (TYRO3), transcript variant X…	Homo s…	human	9606	728	728	53%	0.0	98.54%	4396	XM_017022543.3
Homo sapiens TYRO3 protein tyrosine kinase, mRNA (cDNA clone MGC:51900 IMAGE:6…	Homo s…	human	9606	728	728	53%	0.0	98.54%	3826	BC051756.1
Homo sapiens TYRO3 protein tyrosine kinase, mRNA (cDNA clone IMAGE:4821755)	Homo s…	human	9606	728	728	53%	0.0	98.54%	3759	BC034960.1
Homo sapiens mRNA for TYRO3 protein tyrosine kinase variant protein	Homo s…	human	9606	728	728	53%	0.0	98.54%	3059	AB209431.1
Homo sapiens mRNA for Sky, complete cds	Homo s…	human	9606	728	728	53%	0.0	98.54%	3949	D17517.1

Figure 24. BLAST analysis of Iso-1 TYRO rev seq

Iso 2 with TYRO seq 1 chromatogram

CCGAGATCTCCCAGCCAGTGTGGCTCAGGAAAAAGGaGTGCCATTTTTCACAGTGGA
GCCAAAAGATCTGGCAGTGCCACCCAATGCCCCTTTCCAACTGTCTTGTGAGGCTGT
GGGTCCCCCTGAACCTGTTACCATTGTCTGGTGGAGAGGAACTACGAAGATCGGGGG
ACCCGCTCCCTCTCCATCTGTTTTAAATGTAACAGGGGTGACCCAGAGCACCATGTTT
TCCTGTGAAGCTCACAACCTAAAAGGCCTGGCCTCTTCTCGCACAGCCACTGTTCAC
CTTCAAGCACTGCCTGCAGCCCCCTTCAACATCACCGTGACAAAGCTTTCCAGCAGC
AACGCTAGTGTGGCCTGGATGCCAGGTGCCGATGGCCGAGCTCTGCTACAGTCCTGT
ACAGTTcatGTGacacAGGCCCCAGGAGGCTGGGAAGTCCTGGCTGTTGTGGTCCCTGT
GCCCCCCTTTACCTGCCTGCTCCGGGACCTGGTGCATGCCACCAACTACAGCCTCAG
GGTGCGCTGTGCCAATGCCTTGGGGCCCTCTCCCTAGGCTGACTGGGTGCCCTTTCAG
ACCAAGGGTCTAGCCCCAGCCAGCGCTCCCCAAAACCTCCATGCCATCCGCACAGAT
TCACGCCTCATCTTGGAGTGGGAAGAAGTGATCCCCGAGGCCCCTTTGGAAGGCCCC
CTGGGACCCTACAAACTGTCCTGGGTTCAAGACAATGAAACCCAGGATGAGCTGACA
GTGGAAGGGAACCAGGGCCAATTTGACAGGCTGGGAATCCCCCAAAAGGACCTGAA
TCGTACGTGTGTGCGTCTTCcAAWTGcAGTTGGCTGTGGGAACcCTGCAGTCAGCCcC
TGGGTGGTTCttCTTTCCTCATGGACCGTTGCA

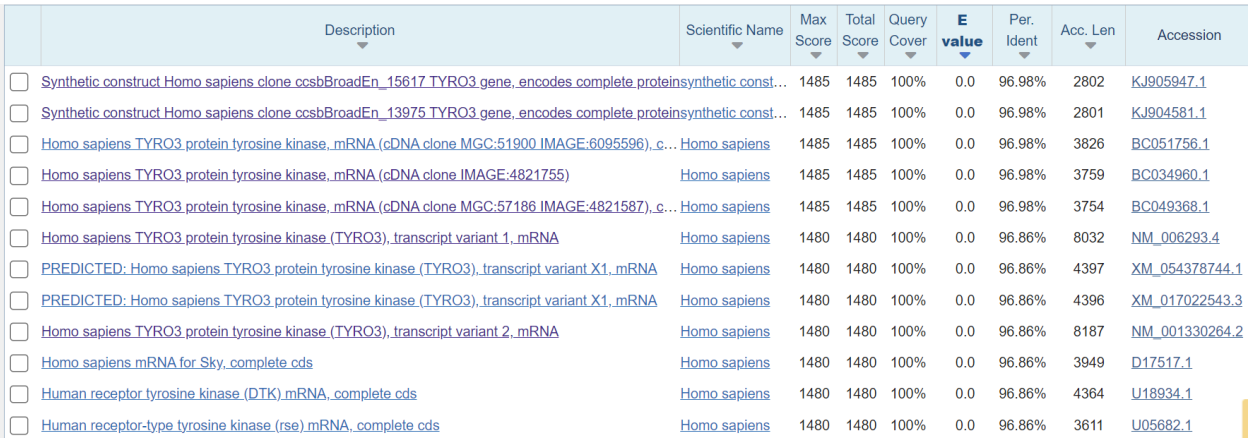

Description	Scientific Name	Max Score	Total Score	Query Cover	E value	Per. Ident	Acc. Len	Accession
Synthetic construct Homo sapiens clone ccsbBroadEn_15617 TYRO3 gene, encodes complete protein	synthetic const…	1485	1485	100%	0.0	96.98%	2802	KJ905947.1
Synthetic construct Homo sapiens clone ccsbBroadEn_13975 TYRO3 gene, encodes complete protein	synthetic const…	1485	1485	100%	0.0	96.98%	2801	KJ904581.1
Homo sapiens TYRO3 protein tyrosine kinase, mRNA (cDNA clone MGC:51900 IMAGE:6095596), c…	Homo sapiens	1485	1485	100%	0.0	96.98%	3826	BC051756.1
Homo sapiens TYRO3 protein tyrosine kinase, mRNA (cDNA clone IMAGE:4821755)	Homo sapiens	1485	1485	100%	0.0	96.98%	3759	BC034960.1
Homo sapiens TYRO3 protein tyrosine kinase, mRNA (cDNA clone MGC:57186 IMAGE:4821587), c…	Homo sapiens	1485	1485	100%	0.0	96.98%	3754	BC049368.1
Homo sapiens TYRO3 protein tyrosine kinase (TYRO3), transcript variant 1, mRNA	Homo sapiens	1480	1480	100%	0.0	96.86%	8032	NM_006293.4
PREDICTED: Homo sapiens TYRO3 protein tyrosine kinase (TYRO3), transcript variant X1, mRNA	Homo sapiens	1480	1480	100%	0.0	96.86%	4397	XM_054378744.1
PREDICTED: Homo sapiens TYRO3 protein tyrosine kinase (TYRO3), transcript variant X1, mRNA	Homo sapiens	1480	1480	100%	0.0	96.86%	4396	XM_017022543.3
Homo sapiens TYRO3 protein tyrosine kinase (TYRO3), transcript variant 2, mRNA	Homo sapiens	1480	1480	100%	0.0	96.86%	8187	NM_001330264.2
Homo sapiens mRNA for Sky, complete cds	Homo sapiens	1480	1480	100%	0.0	96.86%	3949	D17517.1
Human receptor tyrosine kinase (DTK) mRNA, complete cds	Homo sapiens	1480	1480	100%	0.0	96.86%	4364	U18934.1
Human receptor-type tyrosine kinase (rse) mRNA, complete cds	Homo sapiens	1480	1480	100%	0.0	96.86%	3611	U05682.1

Figure 25. BLAST analysis of Iso-2 TYRO seq 1

Iso 2 with TYRO seq 2 chromatogram

GTCCTGGGTTCAAGACAATGGAAAAGAAtGAGCTGACAGTGGAGGGGACCAGGGCC
AATTTGACAGGCTGGGATCCCCAAAAGGACCTGATCGTACGTGTGTGCGTCTCCAAT
GCAGTTGGCTGTGGACCCTGGAGTCAGCCACTGGTGGTCTCTTCTCATGACCGTGCA
GGCCAGCAGGGCCCTCCTCACAGCCGCACATCCTGGGTACCTGTGGTCCTTGGTGTG
CTAACGGCCCTGGTGACGGCTGCTGCCCTGGCCCTCATCCTGCTTCGAAAGAGACGG
AAAGAGACGCGGTTTGGGCAAGCCTTTGACAGTGTCATGGCCCGGGGAGAGCCAGC
CGTTCACTTCCGGGCAGCCCGGTCCTTCAATCGAGAAAGGCCCGAGCGCATCGAGGC
CACATTGGAcAGCTTGGGCATCAGCGATGAACTAAAGGAAAAACTGGAGGATGTGCT
CATCCCAGAGCAGCAGTTCACCCTGGGCCGGATGTTGGGCAAAGGAGAGTTTGGTTC
AGTGCGGGAGGCCCAGCTGAAGCAAGAGGATAGCTCCTTTGTGAAAGTGGCTGTGA
AGATGCTGAAAGCTGACATCATTGCCTCAAGCGACATTGAAGAGTTCCTCAGGGAAG
CAGCTTGCATGAAGGAGTTTGACCATCCACACGTGGCCAAACTTGTTGGGGTAAGCC
TCCGGAGCAGGCTAAAGGCCGTCTCCCCATCCCCCATGGTCATCTTGCCCTTCATGAA
GCATGGGGGACCTGCATGCCTTCCTGCTCGCCTTCCGGATTGGGGAGAACCCCTTTAA
CCTACCCCCTCCAGAAC

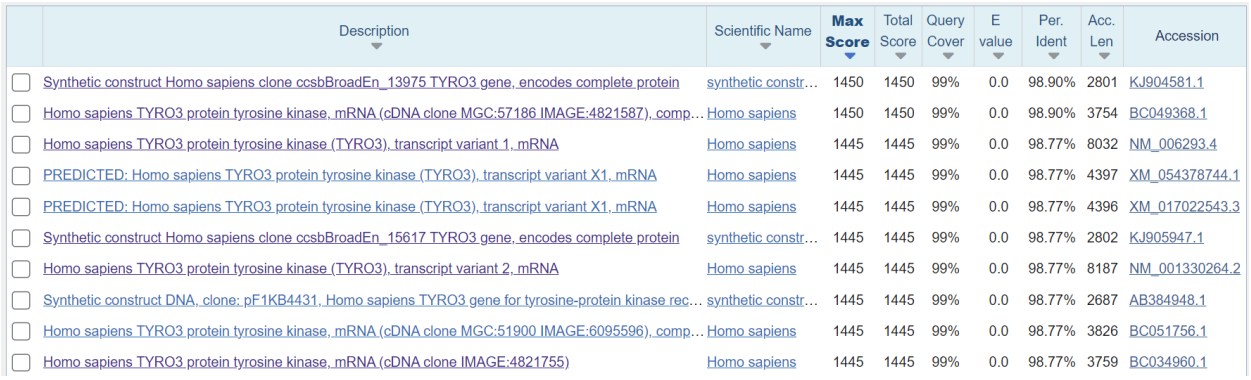

Description	Scientific Name	Max Score	Total Score	Query Cover	E value	Per. Ident	Acc. Len	Accession
Synthetic construct Homo sapiens clone ccsbBroadEn_13975 TYRO3 gene, encodes complete protein	synthetic constr…	1450	1450	99%	0.0	98.90%	2801	KJ904581.1
Homo sapiens TYRO3 protein tyrosine kinase, mRNA (cDNA clone MGC:57186 IMAGE:4821587), comp…	Homo sapiens	1450	1450	99%	0.0	98.90%	3754	BC049368.1
Homo sapiens TYRO3 protein tyrosine kinase (TYRO3), transcript variant 1, mRNA	Homo sapiens	1445	1445	99%	0.0	98.77%	8032	NM_006293.4
PREDICTED: Homo sapiens TYRO3 protein tyrosine kinase (TYRO3), transcript variant X1, mRNA	Homo sapiens	1445	1445	99%	0.0	98.77%	4397	XM_054378744.1
PREDICTED: Homo sapiens TYRO3 protein tyrosine kinase (TYRO3), transcript variant X1, mRNA	Homo sapiens	1445	1445	99%	0.0	98.77%	4396	XM_017022543.3
Synthetic construct Homo sapiens clone ccsbBroadEn_15617 TYRO3 gene, encodes complete protein	synthetic constr…	1445	1445	99%	0.0	98.77%	2802	KJ905947.1
Homo sapiens TYRO3 protein tyrosine kinase (TYRO3), transcript variant 2, mRNA	Homo sapiens	1445	1445	99%	0.0	98.77%	8187	NM_001330264.2
Synthetic construct DNA, clone: pF1KB4431, Homo sapiens TYRO3 gene for tyrosine-protein kinase rec…	synthetic constr…	1445	1445	99%	0.0	98.77%	2687	AB384948.1
Homo sapiens TYRO3 protein tyrosine kinase, mRNA (cDNA clone MGC:51900 IMAGE:6095596), comp…	Homo sapiens	1445	1445	99%	0.0	98.77%	3826	BC051756.1
Homo sapiens TYRO3 protein tyrosine kinase, mRNA (cDNA clone IMAGE:4821755)	Homo sapiens	1445	1445	99%	0.0	98.77%	3759	BC034960.1

Figure 26. BLAST analysis of Iso-2 TYRO seq 2

Iso 2 with TYRO seq 3 chromatogram

GtCCCCATGGtCATAGGACTTcGTGAAGCATGGGGACCTGCATGCCTTCCTGCTCCCCT
CCCGGATTGGGGAGAACCCCTTTAACCTACCCCTCCAGACCCTGATCCGGTTCATGGT
GGACATTGCCTGCGGCATGGAGTACCTGAGCTCTCGGAACTTCATCCACCGAGACCT
GGCTGCTCGGAATTGCATGCTGGCAGAGGACATGACAGTGTGTGTGGCTGACTTCGG
ACTCTCCCGGAAGATCTACAGTGGGGACTACTATCGTCAAGGCTGTGCCTCCAAACT
GCCTGTCAAGTGGCTGGCCCTGGAGAGCCTGGCCGACAACCTGTATACTGTGCAGAG
TGACGTGTGGGCGTTCGGGGTGACCATGTGGGAGATCATGACACGTGttTTTTAcgCCA
TATGCTGGCATCGAAAACGCTGAGATTTACAACTACCTCATTGGCGGGAACCGCCTGA
AACAGCCTCCGGAGTGTATGGAGGACGTGTATGATCTCATGTACCAGTGCTGGAGTGC
TGACCCCAAGCAGCGCCCGAGCTTTACTTGTCTGCGAATGGAACTGGAGAACATCTT
GGGGCCAGCTGTCTGTGCTATCTGCCAGCCAGGACCCCTTATACATCAACATCGAGAG
AGCTGAGGAGCCCACTGCGGGAGGCAGCATGGAGCTACCTGGCGGGGATCAGCCCT
ACAGTGGGGGCTGGGGGATGGCAGTGGCaATGGGGGGCAGTGGGTGGCACTTCCCA
GTGACTGTCGGTAACA

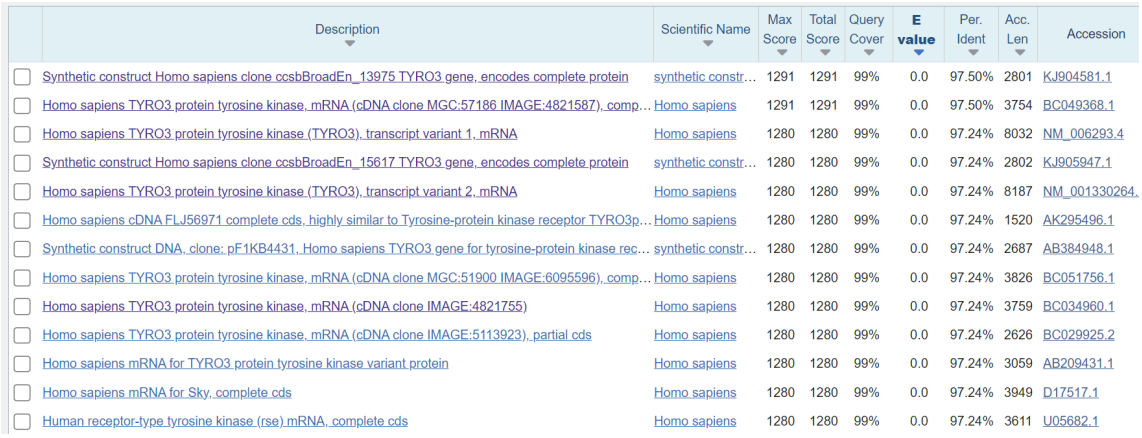

Description	Scientific Name	Max Score	Total Score	Query Cover	E value	Per. Ident	Acc. Len	Accession
Synthetic construct Homo sapiens clone ccsbBroadEn_13975 TYRO3 gene, encodes complete protein	synthetic constr…	1291	1291	99%	0.0	97.50%	2801	KJ904581.1
Homo sapiens TYRO3 protein tyrosine kinase, mRNA (cDNA clone MGC:57186 IMAGE:4821587), comp…	Homo sapiens	1291	1291	99%	0.0	97.50%	3754	BC049368.1
Homo sapiens TYRO3 protein tyrosine kinase (TYRO3), transcript variant 1, mRNA	Homo sapiens	1280	1280	99%	0.0	97.24%	8032	NM_006293.4
Synthetic construct Homo sapiens clone ccsbBroadEn_15617 TYRO3 gene, encodes complete protein	synthetic constr…	1280	1280	99%	0.0	97.24%	2802	KJ905947.1
Homo sapiens TYRO3 protein tyrosine kinase (TYRO3), transcript variant 2, mRNA	Homo sapiens	1280	1280	99%	0.0	97.24%	8187	NM_001330264.
Homo sapiens cDNA FLJ56971 complete cds, highly similar to Tyrosine-protein kinase receptor TYRO3p…	Homo sapiens	1280	1280	99%	0.0	97.24%	1520	AK295496.1
Synthetic construct DNA, clone: pF1KB4431, Homo sapiens TYRO3 gene for tyrosine-protein kinase rec…	synthetic constr…	1280	1280	99%	0.0	97.24%	2687	AB384948.1
Homo sapiens TYRO3 protein tyrosine kinase, mRNA (cDNA clone MGC:51900 IMAGE:6095596), comp…	Homo sapiens	1280	1280	99%	0.0	97.24%	3826	BC051756.1
Homo sapiens TYRO3 protein tyrosine kinase, mRNA (cDNA clone IMAGE:4821755)	Homo sapiens	1280	1280	99%	0.0	97.24%	3759	BC034960.1
Homo sapiens TYRO3 protein tyrosine kinase, mRNA (cDNA clone IMAGE:5113923), partial cds	Homo sapiens	1280	1280	99%	0.0	97.24%	2626	BC029925.2
Homo sapiens mRNA for TYRO3 protein tyrosine kinase variant protein	Homo sapiens	1280	1280	99%	0.0	97.24%	3059	AB209431.1
Homo sapiens mRNA for Sky, complete cds	Homo sapiens	1280	1280	99%	0.0	97.24%	3949	D17517.1
Human receptor-type tyrosine kinase (rse) mRNA, complete cds	Homo sapiens	1280	1280	99%	0.0	97.24%	3611	U05682.1

Figure 27. BLAST analysis of Iso-2 TYRO seq 3

Iso 2 with TYRO seq 4 chromatogram

CTTGTCTGCGAATGGAACTGGAGAAAAAGGGCCGGTGTCTGTGCTATCTGCCAGCCA
GGACCCCTAACAWaaacATCGAGAGAGCTGAGGAGCCCACTGCGGGAGGCAGCATGG
AGCTACCTGGCGGGGATCAGCCCTACAGTGGGGCTGGGGATGGCAGTGGCATGGGG
GCAGTGGGTGGCACTCCCAGTGACTGTCGGTACATACTCACCCCCGGAGGGCTGGCT
GAGCAGCCAGGGCAGGCAGAGCACCAGCCAGAGAGTCCCCTCAATGAGACACAGA
GGCTTTTGCTGCTGCAGCAAGGGCTACTGCCACTCAGTAGCTGTTATCCATATGATGTT
CCAGATTATGCTGAATTCGGATCCGCGGCCGCATAGATAACTGATCCAGTGTGCTGGA
ATTAATTttTCTGTCTTTCgaGGGCCAGCTGTTGGGGTGAGTACTCCCTCTCAAAAGCGG
GCATGACTTCTGcGCTAAGATTGTCAGTTTTCCAAAAACGAGGAGGATTTGATATTCA
CCTGGCCCGCGGGTGATGCCTTTGAGGGTGGCCGCGTCCATCTGGTCAGAAAAGGAC
CAATCTTTTTTGTTGGTCAAGCTTGAGGTGTGGCAGGCTTTGAGAATCTGGCCATACA
CTTtGAGTGGACAATGAaCATCCACTTTTGCCTTTTCTCTCCCACAGGTGTCCACTTCC
CAGGGTCCAACTGCAGGTCGAaGCATGCATCTTAGGGGCGGCCCAATTCCGC

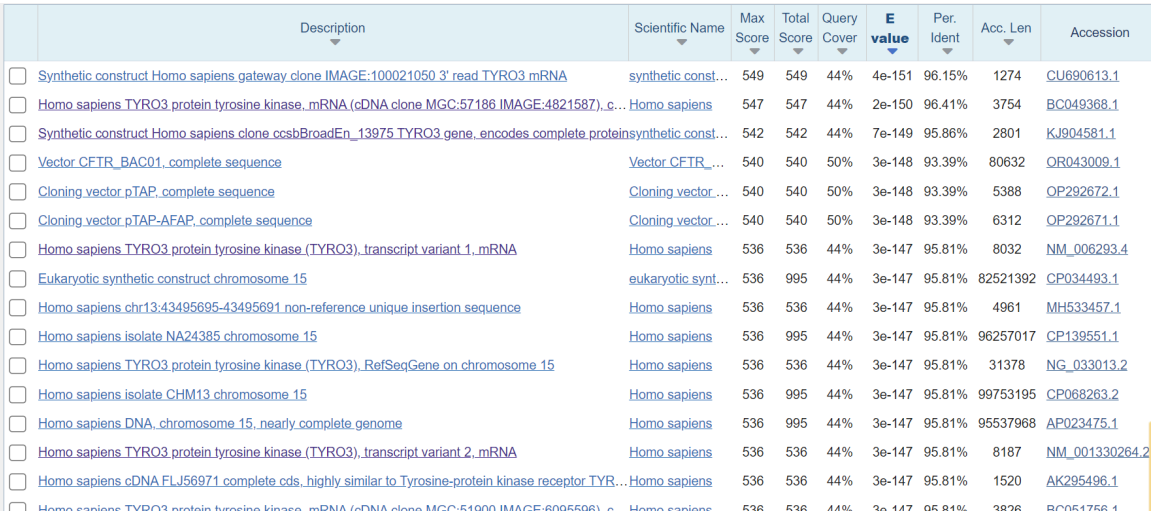

Description	Scientific Name	Max Score	Total Score	Query Cover	E value	Per. Ident	Acc. Len	Accession
Synthetic construct Homo sapiens gateway clone IMAGE:100021050 3' read TYRO3 mRNA	synthetic const…	549	549	44%	4e-151	96.15%	1274	CU690613.1
Homo sapiens TYRO3 protein tyrosine kinase, mRNA (cDNA clone MGC:57186 IMAGE:4821587), c…	Homo sapiens	547	547	44%	2e-150	96.41%	3754	BC049368.1
Synthetic construct Homo sapiens clone ccsbBroadEn_13975 TYRO3 gene, encodes complete protein	synthetic const…	542	542	44%	7e-149	95.86%	2801	KJ904581.1
Vector CFTR_BAC01, complete sequence	Vector CFTR_…	540	540	50%	3e-148	93.39%	80632	OR043009.1
Cloning vector pTAP, complete sequence	Cloning vector …	540	540	50%	3e-148	93.39%	5388	OP292672.1
Cloning vector pTAP-AFAP, complete sequence	Cloning vector …	540	540	50%	3e-148	93.39%	6312	OP292671.1
Homo sapiens TYRO3 protein tyrosine kinase (TYRO3), transcript variant 1, mRNA	Homo sapiens	536	536	44%	3e-147	95.81%	8032	NM_006293.4
Eukaryotic synthetic construct chromosome 15	eukaryotic synt…	536	995	44%	3e-147	95.81%	82521392	CP034493.1
Homo sapiens chr13:43495695-43495691 non-reference unique insertion sequence	Homo sapiens	536	536	44%	3e-147	95.81%	4961	MH533457.1
Homo sapiens isolate NA24385 chromosome 15	Homo sapiens	536	995	44%	3e-147	95.81%	96257017	CP139551.1
Homo sapiens TYRO3 protein tyrosine kinase (TYRO3), RefSeqGene on chromosome 15	Homo sapiens	536	536	44%	3e-147	95.81%	31378	NG_033013.2
Homo sapiens isolate CHM13 chromosome 15	Homo sapiens	536	995	44%	3e-147	95.81%	99753195	CP068263.2
Homo sapiens DNA, chromosome 15, nearly complete genome	Homo sapiens	536	995	44%	3e-147	95.81%	95537968	AP023475.1
Homo sapiens TYRO3 protein tyrosine kinase (TYRO3), transcript variant 2, mRNA	Homo sapiens	536	536	44%	3e-147	95.81%	8187	NM_001330264.2
Homo sapiens cDNA FLJ56971 complete cds, highly similar to Tyrosine-protein kinase receptor TYR…	Homo sapiens	536	536	44%	3e-147	95.81%	1520	AK295496.1
Homo sapiens TYRO3 protein tyrosine kinase, mRNA (cDNA clone MGC:51900 IMAGE:6095596), c…	Homo sapiens	536	536	44%	3e-147	95.81%	3826	BC051756.1

Figure 28. BLAST analysis of Iso-2 TYRO seq 4

Iso 1 with TYRO rev seq chromatogram

CACCTTCTACCGTGAGCCACACTGGGGgGAGATCTcGGTTTCACCCCCATCCTCCACC
TGGCACCAgTACCGGMCGGCGTCAGAGCGCTCCACTGACTTCAGGCTGAGGAAGCC
GATCCAGTGCTGCTCGCTGACTGGGATGTACAACTGGTCCAAGTTCTGGACCACAGC
CCCATCCTTCACCCACTGGATGTCAGGCTCCTCCATCCCCTCCACACTGCAGTTGAGC
TTCACCGGCTGCCCCTGAGACACTGTCAGCTTCACCGGGGCTCCCATGAGCTTCAGA
CCTGCGGCGGCGGACTCCGGGAGCAGCAGAGAAGCCAGAGCCGCCAGCAGCAGCC
CGAGCCGCAGTGGCGGCGGCAGCGGCAGCGGCTGGAGCCCCGGCCGCCCCATGCTC
CTCCTCAGCGCCATgcTagCTAGGCCGCAGATATCGATCCGAGCTCGGTACCAAGCTTG
GGTCTCCCTATAGTGAGTCGTATTAATTTCGATAAGCCAGTAAGCAGTGGGTTCTCTAG
TTAGCCAGAGAGCTCTGCTTATATAGACCTCCCACCGTACACGCCTACCGCCCATTTG
CGTCAATGGGGCGGAGTTGTTACGACATTTTGGAAAGTCCCGTTGATTTTGGTGCCAA
AACAAACTCCCATTGACGTCAATGGGGTGGAGACTTGGAAATCCCCGTGAGTCAAAC
CGCTATCCACGCCATTGATGTACTGCCAAAACCGCATCACCATGGGTAATAGCGATGA
CTAATACGTAaATGTACTGGCC

Description	Scientific Name	Common Name	Taxid	Max Score	Total Score	Query Cover	E value	Per. Ident	Acc. Len	Accession
Synthetic construct Homo sapiens clone ccsbBroadEn_13975 TYRO3 gene, encodes co…	syntheti…	NA	32630	737	737	53%	0.0	98.79%	2801	KJ904581.1
Synthetic construct Homo sapiens gateway clone IMAGE:100021050 5' read TYRO3 mRNA	syntheti…	NA	32630	737	737	53%	0.0	98.79%	1250	CU690612.1
Homo sapiens TYRO3 protein tyrosine kinase, mRNA (cDNA clone MGC:57186 IMAGE:4…	Homo s…	human	9606	734	734	53%	0.0	98.79%	3754	BC049368.1
Synthetic construct Homo sapiens clone ccsbBroadEn_15617 TYRO3 gene, encodes co…	syntheti…	NA	32630	732	732	53%	0.0	98.55%	2802	KJ905947.1
Synthetic construct DNA, clone: pF1KB4431, Homo sapiens TYRO3 gene for tyrosine-pro…	syntheti…	NA	32630	730	730	53%	0.0	98.55%	2687	AB384948.1
Homo sapiens TYRO3 protein tyrosine kinase (TYRO3), transcript variant 1, mRNA	Homo s…	human	9606	728	728	53%	0.0	98.54%	8032	NM_006293.4
PREDICTED: Homo sapiens TYRO3 protein tyrosine kinase (TYRO3), transcript variant X…	Homo s…	human	9606	728	728	53%	0.0	98.54%	4397	XM_054378744.1
PREDICTED: Homo sapiens TYRO3 protein tyrosine kinase (TYRO3), transcript variant X…	Homo s…	human	9606	728	728	53%	0.0	98.54%	4396	XM_017022543.3
Homo sapiens TYRO3 protein tyrosine kinase, mRNA (cDNA clone MGC:51900 IMAGE:6…	Homo s…	human	9606	728	728	53%	0.0	98.54%	3826	BC051756.1
Homo sapiens TYRO3 protein tyrosine kinase, mRNA (cDNA clone IMAGE:4821755)	Homo s…	human	9606	728	728	53%	0.0	98.54%	3759	BC034960.1
Homo sapiens mRNA for TYRO3 protein tyrosine kinase variant protein	Homo s…	human	9606	728	728	53%	0.0	98.54%	3059	AB209431.1
Homo sapiens mRNA for Sky, complete cds	Homo s…	human	9606	728	728	53%	0.0	98.54%	3949	D17517.1

Figure 28. BLAST analysis of Iso-2 TYRO rev seq

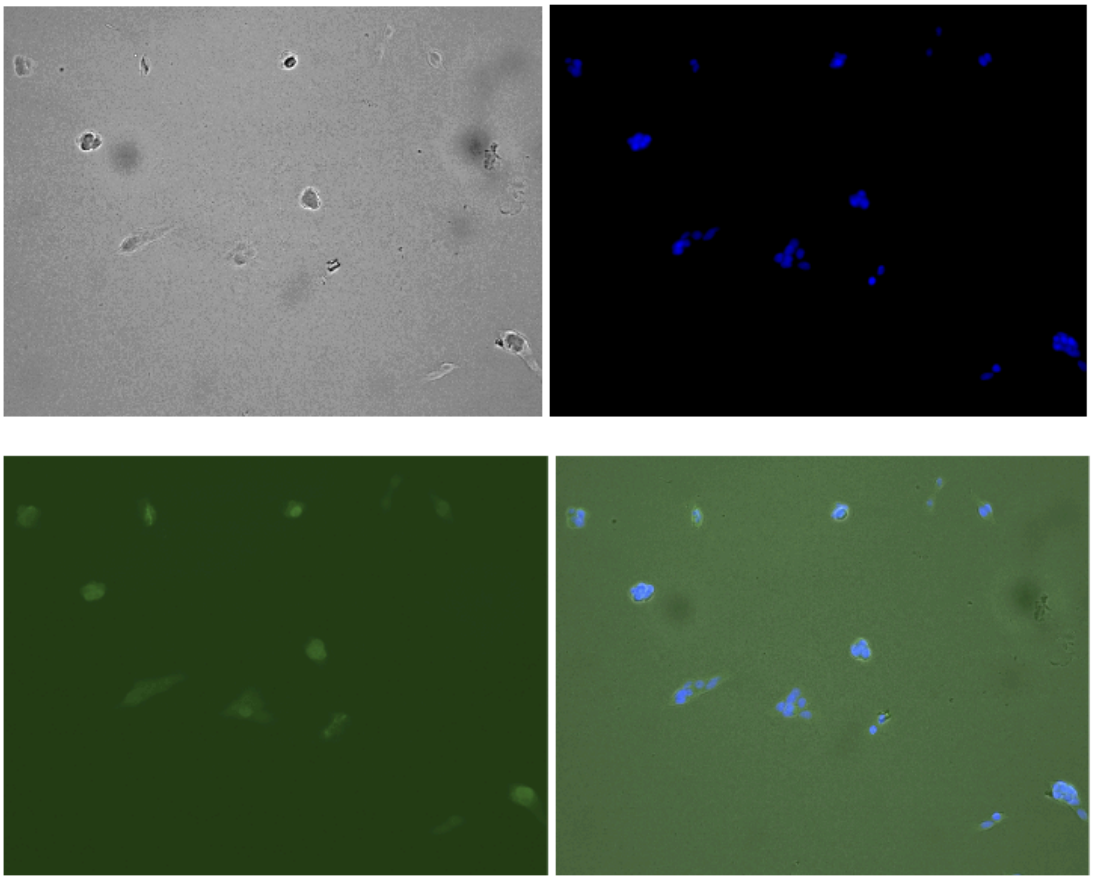

Figure 29. Immunofluorescence of RT112-FRA1-HA tag positive control, DAPI, GFP and transparent channel, 20X magnification. Analyzed by EVOS cell imaging system.

8. REFERENCES

1. World Cancer Research Fund International, Worldwide cancer data, last accessed 17 October 2023, https://www.wcrf.org/cancer-trends/worldwide-cancer-data/
2. National Cancer Institute. (2023, October). Cancer Stat Facts: Bladder Cancer. U.S. Department of Health and Human Services, National Institutes of Health. Retried October 17, 2023 from https://seer.cancer.gov/statfacts/html/urinb.html
3. Amin, M. B., Edge, S. B., Greene, F. L., Byrd, D. R., Brookland, R. K., Washington, M. K., Gershenwald, J. E., Compton, C. C., Hess, K. R., & Sullivan, D. C. (2017). AJCC cancer staging manual (Vol. 1024). Springer.
4. Angelillo-Scherrer, A., de Frutos, P., Aparicio, C., Melis, E., Savi, P., Lupu, F., Arnout, J., Dewerchin, M., Hoylaerts, M., Herbert, J., Collen, D., Dahlbäck, B., & Carmeliet, P. (2001). Deficiency or inhibition of Gas6 causes platelet dysfunction and protects mice against thrombosis. Nature Medicine, 7(2), 215–221. https://doi.org/10.1038/84667
5. Biesecker, L. G., Giannola, D. M., & Emerson, S. G. (1995). Identification of alternative exons, including a novel exon, in the tyrosine kinase receptor gene Etk2/tyro3 that explain differences in 5’ cDNA sequences. Oncogene, 10(11), 2239–2242.
6. Brown, J. E., Krodel, M., Pazos, M., Lai, C., & Prieto, A. L. (2012). Cross-phosphorylation, signaling and proliferative functions of the Tyro3 and Axl receptors in Rat2 cells. PloS One, 7(5), e36800. https://doi.org/10.1371/journal.pone.0036800
7. Compérat, E., Amin, M. B., Cathomas, R., Choudhury, A., De Santis, M., Kamat, A., Stenzl, A., Thoeny, H. C., & Witjes, J. A. (2022). Current best practice for bladder cancer: A narrative review of diagnostics and treatments. The Lancet.
8. Costa, M., Bellosta, P., & Basilico, C. (1996). Cleavage and release of a soluble form of the receptor tyrosine kinase ARK in vitro and in vivo. Journal of Cellular Physiology, 168(3), 737–744.
9. Crittenden, M. R., Baird, J., Friedman, D., Savage, T., Uhde, L., Alice, A., Cottam, B., Young, K., Newell, P., Nguyen, C., Bambina, S., Kramer, G., Akporiaye, E., Malecka, A., Jackson, A., & Gough, M. J. (2016). Mertk on tumor macrophages is a therapeutic target

to prevent tumor recurrence following radiation therapy. Oncotarget, 7(48), 78653–78666. https://doi.org/10.18632/oncotarget.11823

10. Crosier, P. S., Lewis, P. M., Hall, L. R., Vitas, M. R., Morris, C. M., Beier, D. R., Wood, C. R., & Crosier, K. E. (1994). Isolation of a receptor tyrosine kinase (DTK) from embryonic stem cells: Structure, genetic mapping and analysis of expression. Growth Factors, 11(2), 125–136.
11. Crossley, B. M., Bai, J., Glaser, A., Maes, R., Porter, E., Killian, M. L., ... & Toohey-Kurth, K. (2020). Guidelines for Sanger sequencing and molecular assay monitoring. Journal of Veterinary Diagnostic Investigation, 32(6), 767-775.
12. Ding, L., Getz, G., Wheeler, D. A., Mardis, E. R., McLellan, M. D., Cibulskis, K., Sougnez, C., Greulich, H., Muzny, D. M., Morgan, M. B., Fulton, L., Fulton, R. S., Zhang, Q., Wendl, M. C., Lawrence, M. S., Larson, D. E., Chen, K., Dooling, D. J., Sabo, A., … Wilson, R. K. (2008). Somatic mutations affect key pathways in lung adenocarcinoma. Nature, 455(7216), 1069–1075. https://doi.org/10.1038/nature07423
13. Duan, Y., Wong, W., Chua, S. C., Wee, H. L., Lim, S. G., Chua, B. T., & Ho, H. K. (2016). Overexpression of Tyro3 and its implications on hepatocellular carcinoma progression. International Journal of Oncology, 48(1), 358–366. https://doi.org/10.3892/ijo.2015.3244
14. Dufour, F., Silina, L., Neyret-Kahn, H., Moreno-Vega, A., Krucker, C., Karboul, N., Dorland-Galliot, M., Maillé, P., Chapeaublanc, E., & Allory, Y. (2019). TYRO3 as a molecular target for growth inhibition and apoptosis induction in bladder cancer. British Journal of Cancer, 120(5), 555–564.
15. Graham, D. K., DeRyckere, D., Davies, K. D., & Earp, H. S. (2014). The TAM family: Phosphatidylserine-sensing receptor tyrosine kinases gone awry in cancer. Nature Reviews Cancer, 14(12), 769–785.
16. Gehl, J. J. A. P. S. (2003). Electroporation: theory and methods, perspectives for drug delivery, gene therapy and research. Acta Physiologica Scandinavica, 177(4), 437-447.
17. Hafizi, S., & Dahlbäck, B. (2006). Gas6 and protein S. Vitamin K-dependent ligands for the Axl receptor tyrosine kinase subfamily. The FEBS Journal, 273(23), 5231–5244. https://doi.org/10.1111/j.1742-4658.2006.05529.x

18. Heiring, C., Dahlbäck, B., & Muller, Y. A. (2004). Ligand recognition and homophilic interactions in Tyro3: Structural insights into the Axl/Tyro3 receptor tyrosine kinase family. Journal of Biological Chemistry, 279(8), 6952–6958.
19. Jacobsen, K. M., Linger, R. M., & Graham, D. K. (2010). TYRO3 (TYRO3 protein tyrosine kinase). Atlas Genet Cytogenet Oncol Haematol.
20. Jiao, Y., Yonescu, R., Offerhaus, G. J. A., Klimstra, D. S., Maitra, A., Eshleman, J. R., Herman, J. G., Poh, W., Pelosof, L., Wolfgang, C. L., Vogelstein, B., Kinzler, K. W., Hruban, R. H., Papadopoulos, N., & Wood, L. D. (2014). Whole-exome sequencing of pancreatic neoplasms with acinar differentiation. The Journal of Pathology, 232(4), 428–435. https://doi.org/10.1002/path.4310
21. Kariolis, M. S., Miao, Y. R., Jones, D. S., Kapur, S., Mathews, I. I., Giaccia, A. J., & Cochran, J. R. (2014). An engineered Axl'decoy receptor'effectively silences the Gas6-Axl signaling axis. Nature Chemical Biology, 10(11), 977–983.
22. Kasikara, C., Kumar, S., Kimani, S., Tsou, W.-I., Geng, K., Davra, V., Sriram, G., Devoe, C., Nguyen, K.-Q. N., Antes, A., Krantz, A., Rymarczyk, G., Wilczynski, A., Empig, C., Freimark, B., Gray, M., Schlunegger, K., Hutchins, J., Kotenko, S. V., & Birge, R. B. (2017). Phosphatidylserine Sensing by TAM Receptors Regulates AKT-Dependent Chemoresistance and PD-L1 Expression. Molecular Cancer Research: MCR, 15(6), 753–764. https://doi.org/10.1158/1541-7786.MCR-16-0350
23. Kaufman, D. S., Shipley, W. U., & Feldman, A. S. (2009). Bladder cancer. The Lancet, 374(9685), 239–249.
24. Lai, C., Gore, M., & Lemke, G. (1994). Structure, expression, and activity of Tyro 3, a neural adhesion-related receptor tyrosine kinase. Oncogene, 9(9), 2567–2578.
25. Lemke, G. (2013). Biology of the TAM receptors. Cold Spring Harbor Perspectives in Biology, 5(11), a009076.
26. Lew, E. D., Oh, J., Burrola, P. G., Lax, I., Zagórska, A., Través, P. G., Schlessinger, J., & Lemke, G. (2014). Differential TAM receptor-ligand-phospholipid interactions delimit differential TAM bioactivities. eLife, 3, e03385. https://doi.org/10.7554/eLife.03385
27. Lewis, P. M., Crosier, K. E., Wood, C. R., & Crosier, P. S. (1996). Analysis of the murine Dtk gene identifies conservation of genomic structure within a new receptor tyrosine kinase subfamily. Genomics, 31(1), 13–19. https://doi.org/10.1006/geno.1996.0003

28. Linger, R. M., Keating, A. K., Earp, H. S., & Graham, D. K. (2008). TAM receptor tyrosine kinases: Biologic functions, signaling, and potential therapeutic targeting in human cancer. Advances in Cancer Research, 100, 35–83.
29. Magers, M. J., Lopez‐Beltran, A., Montironi, R., Williamson, S. R., Kaimakliotis, H. Z., & Cheng, L. (2019). Staging of bladder cancer. Histopathology, 74(1), 112–134.
30. Mao, S., Wu, Y., Wang, R., Guo, Y., Bi, D., Ma, W., Zhang, W., Zhang, J., Yan, Y., & Yao, X. (2020). Overexpression of GAS6 promotes cell proliferation and invasion in bladder cancer by activation of the PI3K/AKT pathway. OncoTargets and Therapy, 4813–4824.
31. Mark, M. R., Scadden, D. T., Wang, Z., Gu, Q., Goddard, A., & Godowski, P. J. (1994). Rse, a novel receptor-type tyrosine kinase with homology to Axl/Ufo, is expressed at high levels in the brain. The Journal of Biological Chemistry, 269(14), 10720–10728.
32. Paolino, M., Choidas, A., Wallner, S., Pranjic, B., Uribesalgo, I., Loeser, S., Jamieson, A. M., Langdon, W. Y., Ikeda, F., Fededa, J. P., Cronin, S. J., Nitsch, R., Schultz-Fademrecht, C., Eickhoff, J., Menninger, S., Unger, A., Torka, R., Gruber, T., Hinterleitner, R., … Penninger, J. M. (2014). The E3 ligase Cbl-b and TAM receptors regulate cancer metastasis via natural killer cells. Nature, 507(7493), 508–512. https://doi.org/10.1038/nature12998
33. Pastore, M., Grimaudo, S., Pipitone, R. M., Lori, G., Raggi, C., Petta, S., & Marra, F. (2019). Role of myeloid-epithelial-reproductive tyrosine kinase and macrophage polarization in the progression of atherosclerotic lesions associated with nonalcoholic fatty liver disease. Frontiers in Pharmacology, 10, 604.
34. Potter, H., & Heller, R. (2018). Transfection by electroporation. Current protocols in molecular biology, 121(1), 9-3.
35. Rothlin, C. V., Carrera-Silva, E. A., Bosurgi, L., & Ghosh, S. (2015). TAM receptor signaling in immune homeostasis. Annual Review of Immunology, 33, 355–391. https://doi.org/10.1146/annurev-immunol-032414-112103
36. Sadahiro, H., Kang, K.-D., Gibson, J. T., Minata, M., Yu, H., Shi, J., Chhipa, R., Chen, Z., Lu, S., Simoni, Y., Furuta, T., Sabit, H., Zhang, S., Bastola, S., Yamaguchi, S., Alsheikh, H., Komarova, S., Wang, J., Kim, S.-H., … Nakano, I. (2018). Activation of the Receptor Tyrosine Kinase AXL Regulates the Immune Microenvironment in

Glioblastoma. Cancer Research, 78(11), 3002–3013. https://doi.org/10.1158/0008-5472.CAN-17-2433

37. Sasaki, T., Knyazev, P. G., Clout, N. J., Cheburkin, Y., Göhring, W., Ullrich, A., Timpl, R., & Hohenester, E. (2006). Structural basis for Gas6-Axl signalling. The EMBO Journal, 25(1), 80–87. https://doi.org/10.1038/sj.emboj.7600912
38. Sather, S., Kenyon, K. D., Lefkowitz, J. B., Liang, X., Varnum, B. C., Henson, P. M., & Graham, D. K. (2007). A soluble form of the Mer receptor tyrosine kinase inhibits macrophage clearance of apoptotic cells and platelet aggregation. Blood, 109(3), 1026–1033. https://doi.org/10.1182/blood-2006-05-021634
39. Schulz, A. S., Schleithoff, L., Faust, M., Bartram, C. R., & Janssen, J. W. (1993). The genomic structure of the human UFO receptor. Oncogene, 8(2), 509–513.
40. Seitz, H. M., Camenisch, T. D., Lemke, G., Earp, H. S., & Matsushima, G. K. (2007). Macrophages and dendritic cells use different Axl/Mertk/Tyro3 receptors in clearance of apoptotic cells. Journal of Immunology (Baltimore, Md.: 1950), 178(9), 5635–5642. https://doi.org/10.4049/jimmunol.178.9.5635
41. Seshagiri, S., Stawiski, E. W., Durinck, S., Modrusan, Z., Storm, E. E., Conboy, C. B., Chaudhuri, S., Guan, Y., Janakiraman, V., Jaiswal, B. S., Guillory, J., Ha, C., Dijkgraaf, G. J. P., Stinson, J., Gnad, F., Huntley, M. A., Degenhardt, J. D., Haverty, P. M., Bourgon, R., … de Sauvage, F. J. (2012). Recurrent R-spondin fusions in colon cancer. Nature, 488(7413), 660–664. https://doi.org/10.1038/nature11282
42. Shibue, T., & Weinberg, R. A. (2017). EMT, CSCs, and drug resistance: The mechanistic link and clinical implications. Nature Reviews Clinical Oncology, 14(10), 611–629.
43. Siegel, R. L., Miller, K. D., Fuchs, H. E., & Jemal, A. (2022). Cancer statistics, 2022. CA: A Cancer Journal for Clinicians, 72(1), 7–33. https://doi.org/10.3322/caac.21708
44. Siegel, R. L., Miller, K. D., Wagle, N. S., & Jemal, A. (2023). Cancer statistics, 2023. CA: A Cancer Journal for Clinicians, 73(1), 17–48. https://doi.org/10.3322/caac.21763
45. Silina, L., Dufour, F., Rapinat, A., Reyes, C., Gentien, D., Maksut, F., Radvanyi, F., Verrelle, P., Bernard-Pierrot, I., & Mégnin-Chanet, F. (2022). Tyro3 targeting as a radiosensitizing strategy in bladder cancer through cell cycle dysregulation. International Journal of Molecular Sciences, 23(15), 8671.

46. Smart, S. K., Vasileiadi, E., Wang, X., DeRyckere, D., & Graham, D. K. (2018). The Emerging Role of TYRO3 as a Therapeutic Target in Cancer. Cancers, 10(12), 474. https://doi.org/10.3390/cancers10120474
47. Sung, H., Ferlay, J., Siegel, R. L., Laversanne, M., Soerjomataram, I., Jemal, A., & Bray, F. (2021). Global cancer statistics 2020: GLOBOCAN estimates of incidence and mortality worldwide for 36 cancers in 185 countries. CA: A Cancer Journal for Clinicians, 71(3), 209–249.
48. Thorp, E., Vaisar, T., Subramanian, M., Mautner, L., Blobel, C., & Tabas, I. (2011). Shedding of the Mer tyrosine kinase receptor is mediated by ADAM17 protein through a pathway involving reactive oxygen species, protein kinase Cδ, and p38 mitogen-activated protein kinase (MAPK). The Journal of Biological Chemistry, 286(38), 33335–33344. https://doi.org/10.1074/jbc.M111.263020
49. Uehara, S., Fukuzawa, Y., Matuyama, T., & Gotoh, K. (2022). Roles of soluble TAM receptors, ligands for these receptors, and shedding enzymes in patients with acute pancreatitis.
50. van der Meer, J. H., van der Poll, T., & van ‘t Veer, C. (2014). TAM receptors, Gas6, and protein S: roles in inflammation and hemostasis. Blood, The Journal of the American Society of Hematology, 123(16), 2460–2469.
51. Varnum, B. C., Young, C., Elliott, G., Garcia, A., Bartley, T. D., Fridell, Y. W., Hunt, R. W., Trail, G., Clogston, C., & Toso, R. J. (1995). Axl receptor tyrosine kinase stimulated by the vitamin K-dependent protein encoded by growth-arrest-specific gene 6. Nature, 373(6515), 623–626. https://doi.org/10.1038/373623a0
52. Wagle, N., Van Allen, E. M., Treacy, D. J., Frederick, D. T., Cooper, Z. A., Taylor-Weiner, A., Rosenberg, M., Goetz, E. M., Sullivan, R. J., Farlow, D. N., Friedrich, D. C., Anderka, K., Perrin, D., Johannessen, C. M., McKenna, A., Cibulskis, K., Kryukov, G., Hodis, E., Lawrence, D. P., … Garraway, L. A. (2014). MAP kinase pathway alterations in BRAF-mutant melanoma patients with acquired resistance to combined RAF/MEK inhibition. Cancer Discovery, 4(1), 61–68. https://doi.org/10.1158/2159-8290.CD-13-0631
53. Wang, H., Chen, Y., Ge, Y., Ma, P., Ma, Q., Ma, J., Wang, H., Xue, S., & Han, D. (2005). Immunoexpression of Tyro 3 family receptors—Tyro 3, Axl, and Mer—And their ligand

Gas6 in postnatal developing mouse testis. The Journal of Histochemistry and Cytochemistry: Official Journal of the Histochemistry Society, 53(11), 1355–1364. https://doi.org/10.1369/jhc.5A6637.2005

54. Wee, P., & Wang, Z. (2017). Epidermal growth factor receptor cell proliferation signaling pathways. Cancers, 9(5), 52.
55. Weng, C.-H., Chen, L.-Y., Lin, Y.-C., Shih, J.-Y., Lin, Y.-C., Tseng, R.-Y., Chiu, A.-C., Yeh, Y.-H., Liu, C., & Lin, Y.-T. (2019). Epithelial-mesenchymal transition (EMT) beyond EGFR mutations per se is a common mechanism for acquired resistance to EGFR TKI. Oncogene, 38(4), 455–468.
56. Yamagata, M., Sanes, J. R., & Weiner, J. A. (2003). Synaptic adhesion molecules. Current Opinion in Cell Biology, 15(5), 621–632.